

ISSUES ON FINITE ELEMENT MODELING OF LAMINATED COMPOSITE STRUCTURES

by

FARHAN ALAMGIR

Presented to the Faculty of the Graduate School of
The University of Texas at Arlington in Partial Fulfillment
of the Requirements
for the Degree of

MASTER OF SCIENCE IN MECHANICAL ENGINEERING

THE UNIVERSITY OF TEXAS AT ARLINGTON

May 2011

Copyright © by Farhan Alamgir 2010

All Rights Reserved

ACKNOWLEDGEMENTS

I would like to express my appreciation and gratitude to my supervising professor, Dr. Wen S. Chan for his support, and encouragement throughout my research in every aspect and for helping me to develop my base in composite structures. He has been very patient, and extended excellent guidance, never accepting less than my best efforts. This thesis would not have been completed without his inspiration and continuous round the clock support.

I also like to extend my appreciation to my committee members Dr. Kent Lawrence, Dr. Asfaq Adnan for reviewing my thesis and providing guidance during this work. Thanks to Dr. Lawrence for building up my fundamental knowledge in Finite Element.

I would like to thank all former and present students in Dr. Chan's group. We worked as a family I would also like to thank Dr Tan for her contribution.

I would also like to thank entire faculty of Mechanical and Aerospace Engineering for their help in building by understanding of the subject and in preparation of this thesis.

Most of all thanks to my parents Jahangir Mia and Ferdaus Ara Begum, my beloved wife Farzin Ahmed and my brother Fahim Alamgir for their support, sacrifice and encouragement. Without their contribution none of this research would have proceeded.

Finally I like to dedicate my thesis in memory of those who died in Tsunami in Japan.

April 13, 2011

ABSTRACT

ISSUES ON FINITE ELEMENT MODELING OF LAMINATED COMPOSITE STRUCTURES

Farhan Alamgir, M.S

The University of Texas at Arlington, 2010

Supervising Professor: Wen S. Chan

Composite structures have been used widely in aviation industries and civil construction field because of their high specific stiffness, high specific strength and directional dependent properties. When using finite element method to analyze these structures, special attention of modeling is required. This thesis addresses the effect of layer stresses and displacements of a laminate under loading due to element meshing, boundary constraints and material properties used in modeling of composite structures. This study also includes the investigation of the magnitude and location of the layer peak stresses on modeling the laminate with a hole. It is concluded that special characteristics of composite structures such as symmetrical/unsymmetrical and balanced/unbalanced laminate configurations need to be considered in the application of finite element method to composite structures.

TABLE OF CONTENTS

ACKNOWLEDGEMENTS	iii
ABSTRACT.....	iv
LIST OF ILLUSTRATIONS.....	vii
LIST OF TABLES.....	ix
Chapter	Page
1. INTRODUCTION	1
1.1 Overview of composite materials in Structural Applications.....	1
1.2 Finite element modeling of composite structures.....	2
1.3 Issues considered in this study	4
1.4 Objective of the thesis	6
1.5 Outline of the thesis	6
2. REVIEW OF CONSTITUTIVE EQUATIONS OF LAMINATED STRUCTURES	7
2.1 Stiffness matrix of anisotropic materials.....	7
2.2 Mid Plane Strain and Curvature of a Laminate	10
2.3 Constitutive Equation of a Laminate	13
2.4 Laminated beam with rectangular Cross sections	17
2.4.1 Axial Stiffness	17
2.4.2 Bending Stiffness.....	18
2.5 Laminated Rectangular beam with Stacking Sequence Consideration	18
2.5.1 Narrow Beam.....	19
2.5.2 Wide Beam.....	21

2.6 Laminated beam with Curved Cross sections	22
3. FINITE ELEMENT MESHING	26
3.1 Choosing proper mesh size	28
3.2 Auto meshing	31
3.3 Aspect Ratio.....	33
4. ONE DIMENTIONAL, TWO DIMENTIONAL THREE DIMENTIONAL MODELING ...	38
4.1 One Dimensional Model	42
4.2 Two and Three Dimensional Model	46
4.3 Full and Quarter Of Three- Dimensional Models	49
4.4 Full and Quarter Of Two- Dimensional Models of Laminate with a Hole	51
4.5 Lumping Layer Theory	67
5. BOUNDARY CONSTRAINTS	70
5.1 Structural Response of 2D model	70
5.2 Maximum stress of laminate with hole by full 3D and a quarter 3D	71
5.3 Effect of boundary constraints locations	73
5.4 Curved beam with symmetric layup [$\pm 45/0/90$]s	79
6. CONCLUSIONS	83
APPENDIX	
A. FEM MODELS USED IN THE THESIS	85
B. LAMINATION THEORY PROGRAM FOR FLATE PLATE AND CURVED BEAM.....	94
REFERENCES	104
BIOGRAPHICAL INFORMATION.....	106

LIST OF ILLUSTRATIONS

Figure	Page
2.1 k^{th} layer of a Composite Laminated Plate	8
2.2 Fiber Orientation and Coordinate Transformation	9
2.3 Laminated plate.....	11
2.4 Load on a composite laminated plate.....	14
2.5 Layer orientation of a composite plate.	16
2.6 Narrow Beam	19
2.7 Wide Beam	21
2.8 Curved Beam	23
3.1 Different Kind Of Mesh	27
3.2 Circular Cut-out	29
3.3 Different Mesh Size	30
3.4 Free Versus Mapped Mesh	32
3.5 Aspect Ratio	34
4.1 Shell 99 Element.....	40
4.2 Simply Supported Beam	44
4.3 Plate in tension	46
4.4 Deformation of 2d plate with a hole full model	56
4.5 Maximum stress of 2d plate with a hole full model	57
4.6 Deformation of 2d plate with a hole quarter model	57
4.7 Maximum stress of 2d plate with a hole quarter model	59
4.8 Maximum stress of 45 degree lamina in with a hole 2D quarter model	59

4.9 Deformed Shape of 3D Plate with Hole model	63
4.10 Maximum stress of 3d plate with a hole full model (x directional load)	65
4.11 Maximum stress of 3d plate with a hole quarter model (x directional load)	66
5.1 Stress Concentration Comparisons of Quarter and Full 3D Model.....	72
5.2 2D quarter model maximum stress in x direction for positive 45 degree layer	73
5.3 2D quarter model maximum stress in x direction for negative 45 degree layer.....	74
5.4 45 degree layup in full model becomes - 45 degree in 2 nd quadrant quarter model.....	76
5.5 3D quarter model maximum stress in x direction for positive 45 degree layer	77
5.6 quarter model maximum stress in x direction for negative 45 degree layer	77
5.7 3D curved beam	79

LIST OF TABLES

Table	Page
3.1 Results for a 3D Plate with Different Mesh Type	27
3.2 Mesh size results for a 2D Plate with a hole.....	31
3.3 Free versus mapped Mesh for a 2D Plate with a hole	33
3.4 Aspect Ratio Results of a Flat Plate.....	35
4.1 Elements with composite capability in Ansys	39
4.2 Material properties used in this Study	44
4.3 Equivalent modulus	45
4.4 Conventional versus Modified FEM beam deflection	45
4.5 Geometry of 2D full model and 2D quarter model	46
4.6 Comparison between 2d Symmetric full model and quarter model	48
4.7 Comparison between 2d Un- Symmetric full model and quarter model.....	49
4.8 Comparison between 3d Symmetric full model and quarter model	50
4.9 Comparison between 3d Un- Symmetric full model and quarter model.....	51
4.10 Comparison between 2d Symmetric full model and quarter model (notched)	52
4.11 2D Symmetric full model in x-y direction and fiber direction	53
4.12 2D Un-Symmetric full model and quarter model (notched)	54
4.13 Comparison between 2d Un-Symmetric full model in fiber and x-y direction (notched)	55
4.14 Location of maximum stress for 2d symmetric full model.....	56
4.15 Location of maximum stress for 2d symmetric quarter model	58
4.16 Comparison between 3d Symmetric full model and quarter model (notched).....	60

4.17 3D Symmetric full model stress in fiber direction	61
4.18 Peak stress location of 3D symmetric full model in fiber direction	62
4.19 Comparison between 3d Un- Symmetric full model and quarter model	63
4.20 Comparison between 3d Un- Symmetric full model in fiber and x-y direction	64
4.21 Location of maximum stress for 3d symmetric full model in fiber direction	65
4.22 Location of maximum stress for 3d symmetric full and quarter model	66
4.23 Equivalent Property Table for Lumped Layers	67
4.24 Lumping Layer Technique Table.....	68
4.25 Lumping Layer Recovery Technique Table.....	69
5.1 Comparison of Normalized Displacement	71
5.2 Stress distribution to show symmetric constraint effect	72
5.3 2D quarter swap effect	75
5.4 3D quarter swap effect	78
5.5 Curvature effect for 3d Curved Beam model	80
5.6 Curved Beam aspect ratio comparison	81
5.7 2D and 3D curved beam comparison	82
5.8 curved beam aspect ratio comparison	82

CHAPTER 1

INTRODUCTION

1.1 Overview of composite materials in Structural Applications

Composites are materials made from two or more constituent materials with significantly different physical or chemical properties which remain separate and distinct at the macroscopic or microscopic scale within the finished structure. One of the materials is discontinuous and stiffer and stronger called the reinforcement, whereas the less stiff material is called the matrix.

Advanced composite are becoming more widely used as an alternative to metallic structures. Since boron and graphite fibers were first developed in the early 1960's, application of advanced composites in military aircrafts have accelerated rapidly. The basic advantage of using composite materials over metals is in their high strength to weight and stiffness to weight properties, which have great potential for reducing structural weight.

Applications of composites have been extended widely to the aircraft, marine, automotive, sporting goods, biomedical industries, civil constructions and many other fields. Increasing use of composite in structures are also required an understanding of their structural responses and failure mechanisms. Unlike isotropic materials, composite structures exhibits complicated anisotropic behavior, such as tension/shear coupling and tension/bending coupling as well as bending twisting coupling. Although the history of using composite materials is very old, stress analysis of composite structures is relatively new. Composite structure is often made by laminating the composite layers (so-called "lamina") together with the different fiber orientation according to the requirement of load. The lamina in general, is a thin layer and is

inherent of not isotropic structural behavior. A theory of laminated plate, so-called “classical lamination theory”, was developed in 1960s in analyzing the stress/strain of each lamina. This theory assumes that the state of stress within each lamina of a multidirectional laminate is planar. However this assumption is not true in the vicinity of free edge. The variation in material properties between layers of laminated composites can produce significant inter-laminar stresses. This inter-laminar stress is three dimensional even in a very thin plate. Hence, analyses using lamination plate theory, which assumes a plane stress condition, is not applicable in the neighborhood of the free edge.

In short, analysis of composite structures requires knowledge of anisotropic elasticity. Most problems involving composite structures do not admit exact solution; therefore finite element method is used to find approximate but representative solutions.

This method is a well developed numerical tool available today for predicting the response of composite structures. Throughout the year, the scope of finite element analysis has always been closely related to the advancement of computers and computational techniques. The development of advanced super computers and even affordable personal computers provide effective resources to solve complicated problems.

1.2 Finite element modeling of composite structures

Finite element (FE) analysis is an alternative approach to solve the governing equations of any structural problem. Classical (continuum) methods of stress analysis can be applied satisfactorily for solving structural problems to some extent. These analyses are based on the application of the equations of equilibrium and compatibility, together with the stress-strain relations for the material, to produce governing equations which must be solved to obtain displacements and stresses. There is always some assumptions that must be made before the solution can be effected. In case of composites generally two common theories, namely Classical plate theory (CLT) and First order shear deformation plate theory (FSDT) are used.

These theories are not always applicable for all structural problems. If the geometry of

the structural problem is not simple, say it moves away from a plain rectangular plate to one containing cut-out, the governing equations become increasingly complicated and require ever more sophisticated mathematical techniques to solve them. As a result the adoption of FE analyses is quite obvious.

The FE method consists of dividing the structure to be composed of discrete parts, which are then assembled in such a way as to represent the distortion of the structure under specified loads. Each element has an assumed displacement field. The FE method was initially developed for isotropic materials and the majority of the elements available (“in library”) in any software package would be for such materials. To apply the technique to composites requires special attentions.

Extensive research has been done using FEM technique on analyze composite structures with and without a cutout. Among the book publications, Reddy and Ochoa [1] was the first textbook focused on composite laminate analysis by using finite element method. Several bench mark examples have been demonstrated. Recently, Strong [2] in his book discussed the special issues that must be considered when using the finite element method to analyze composite materials and structures. Barbero [3] focused on the composite analysis by using ANSYS. In those books, some of special issues in modeling composite structures were still not addressed.

Since most of composite structures are the thin compared to the other dimensions of the structures, it is logically to model the structures using 2-dimensional plate or shell element. Because of the different properties of each layer, the properties used in the plate or shell element are often obtained the smeared in-plane properties buy using lamination theory. In doing so, the inter-laminar stresses which exit near the free edge are not able to directly obtain. In order to obtain a full state of stresses, stacking three-dimensional element (for example, brick element) with one or two elements representing a ply of composite materials are often

conducted. However, an accurate three dimensional analysis introduces a larger number of degree of freedom resulting in enormous memory and computational time requirement. Because of thin layer, maintaining a proper aspect ratio of finite element results in an increased number of elements in the model. As a consequence, layering brick elements through the thickness of relatively thin plates leads to very ill-conditioned sets of equations. This makes the program very expensive to run. It is also impractical to consider individual lamina, which are located far from the region of interest. Hence a group of laminas are often lumped together into a single layer of an equivalent 0^0 layer to reduce the size of the problem in finite element analysis. In doing so, the use of effective moduli for replacing the lumped heterogeneous medium by an equivalent homogeneous material is required.

A number of methods have been reported in the literature for computing the effective moduli of a laminate. The in-plane elastic constants were obtained from Classical Lamination Theory. But the effect of curvature and shear deformation on the effective moduli was ignored if un-symmetric and un-balanced lamias were lumped together. Chen and Chan [4] proposed a method for calculating equivalent properties of the lumped layer to account those coupling effects. Later, Lin, al. et. [5] developed an expression for equivalent thermal expansion coefficients of lumped layer in laminated composites.

Many works have been done modeling a laminate with a hole. Because of symmetry of loading and global laminate configuration, a quarter or half structure of the entire laminate was often taken for model. These symmetry conditions violate the symmetry of material axis.

The main purpose of this thesis is to discuss the special issues that must be considered when using the FE method to analyze composite materials and structures.

1.3 Issues considered in this study

While modeling of a composite material structure special consideration should be made on material selection, or choosing material constants, meshing technique, boundary conditions,

modeling dimensions (1- dimension, 2-dimension or 3-dimension), lay-up properties of composites.

As composite materials are inherently anisotropic it needs four properties young's modulus in fiber directions, young's modulus transverse to the fiber direction , in plane shear modulus and in plane poisons ratio. So selecting a proper element that supports all the material property issues of a composite material is of a prime consideration.

Composites have directional properties. It is designed to exploit an improvement in mechanical properties. Both the constituent present in a composite has distinct characteristics which develops the continuum of the structure. So accuracy of the FEM solution largely depends on the choice of mesh. If the selected mesh violates the symmetry of the problem, the resulting solution will be less accurate than one aligned with the symmetry of the problem. This is the so-called effect of the geometric isotropy. If triangular element is used for meshing, as it is suitable for representing any geometrical complexity because of their complete polynomial representation, geometrical anisotropy may arise. That may leads to an erroneous stress analyses of the composite model.

Boundary condition is another issue that needs special consideration. Unlike isotropic materials, depending on its layup (symmetric or un-symmetric, balanced or unbalanced) composite may behave in a unconventional way when load is applied. For an example, if simple tension load is applied on a cantilever beam made of isotropic material, the displacement is always in load direction, but for a composite material the type of deflection may vary depending on the layup. So if there is an out-of-plane deflection it is not recommended to constrain the degree of freedom at that direction. So boundary condition plays a special role while modeling a composite material.

Special consideration should be taken depending on the modeling dimensions and layup of a composite material.

1.4 Objective of the thesis

The main purpose of the thesis is to investigate the special issues that are needed to pay special attention when using finite element method in analyzing composite structures. The particular issues illustrated through the examples taken from the particular problems. This study is not intended to compare the types of elements used in modeling composite structure but to emphasize the effect of the results due to the issues described in the previous section. It is believed that those issues were not widely pointed out in composite structure modeling.

1.5 Outline of the thesis

Chapter 2 is a review of constitutive equations of laminated structures. Mainly the development of stiffness matrix of a laminate is described, followed by a brief review of Classical plate theory and laminated beam equations with rectangular and curved sections.

Chapter 3 presents the Finite element meshing techniques, geometrical isotropy and auto meshing.

Chapter 4 presents One-dimensional, two dimensional and three-dimensional modeling.

The effect of the stress results due to the boundary conditions on finite element modeling is discussed in Chapter 5.

Conclusions and recommendation drawn from this study are included in Chapter 6.

CHAPTER 2

REVIEW OF CONSTITUTIVE EQUATIONS OF LAMINATED STRUCTURES

In structural applications, composite materials are used in the form of thin laminates which are constructed by stacking multiple laminas together. Instead of analyzing layer by layer stress individually, the mid- plane of laminate is selected as a reference plane. Then the in-plane structural properties of each ply are transferred into this plane. This type of analysis method is called “Lamination Theory”. This chapter reviews the lamination theory that has been used to calculate the ply stress and strain for a given laminated plate. Extension of the lamination theory to a straight and curved beam is also reviewed.

2.1 Stiffness matrix of anisotropic materials

Classical Lamination theory describes the stress and deformation hypothesis to analyze the behavior of laminated plate. By the use of this theory, we can consistently precede from the basic lamina to the end result the structural laminate. The whole process is one of finding effective and reasonably accurate simplifying assumptions that enable us to reduce our attention from a complicated three dimensional elasticity problem to a solvable two dimensional mechanics of deformable bodies' problem.

To calculate the mechanical properties of composites it is convenient to start by considering a composite in which all the fibers are located in one dimension (unidirectional composite). This basic building block can then be used to predict the behavior of continuous fiber multidirectional laminates. The following figure 2.1 is showing a laminated plate. A k^{th} layer represents a lamina at z distance from the mid plane.

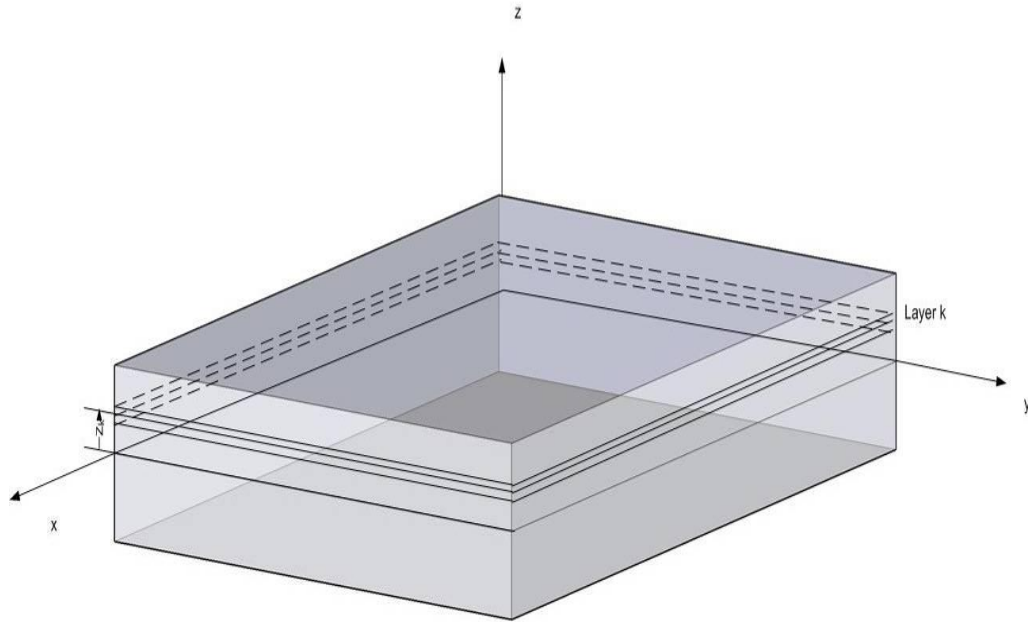


Figure 2.1 k^{th} layer of a Composite Laminated Plate

We will first discuss the stress –strain behavior of an individual lamina and express the equation for the k^{th} lamina of a laminate. We have the following assumptions:

1. Each layer (Lamina) of the laminate is quasi homogeneous and orthotropic
2. The laminate is thin; this means the lateral dimension is much larger than its thickness. So Plane Stress condition is used.

3. All displacements are small compared with the thickness of the laminate

Using these assumptions the problem is now a two dimensional problem. Now similar to the above figure this plate like entities are often constructed by assembling layers (or lamina or plies), usually unidirectional, one on top of another, the direction of fibers normally being changed from layer to layer. Consequently there will be layers for which the fibers are no longer aligned with the applied stresses. These are termed as rotated layers and can be said that they are subjected to off-axis loading.

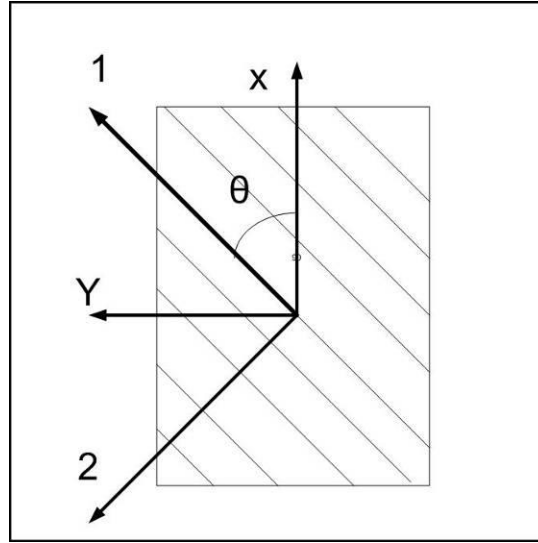


Figure 2.2 Fiber orientation and co-ordinate transformation

The above fig 2.2 shows the co-ordinate system of a single lamina. The global coordinate system is represented by x-y and Fiber coordinate system is represented by 1-2 direction where 1 is parallel to the fiber direction and 2 is transverse to the fiber direction. The stress-strain relations in the principle material coordinates in 1-2 direction for a lamina under plane stress are,

$$\begin{pmatrix} \sigma_1 \\ \sigma_2 \\ \tau_{12} \end{pmatrix} = \begin{pmatrix} Q_{11} & Q_{12} & 0 \\ Q_{12} & Q_{22} & 0 \\ 0 & 0 & Q_{66} \end{pmatrix} \begin{pmatrix} \varepsilon_1 \\ \varepsilon_2 \\ \gamma_{12} \end{pmatrix} \quad (2.1)$$

Where, [Q] is called the reduced stiffness matrix and the values of different element of [Q] matrix are as follows,

$$Q_{11} = \frac{E_1}{1 - \nu_{12}\nu_{21}}, \quad Q_{22} = \frac{E_2}{1 - \nu_{12}\nu_{21}}, \quad Q_{12} = \frac{\nu_{12}E_1}{1 - \nu_{12}\nu_{21}} = \frac{\nu_{21}E_2}{1 - \nu_{12}\nu_{21}}, \quad Q_{66} = G_{12}$$

The stiffness matrix $[\bar{Q}_{x-y}]$ for a lamina with fiber rotation of an arbitrary angle θ with respect to global axis can be obtained by rotating the stiffness matrix of a 0° lamina $[Q_{1-2}]$, as

shown in the following equation.

$$[\bar{Q}_{x-y}] = [T_{\sigma}(-\vartheta)][Q_{1-2}][T_{\varepsilon}(\vartheta)] \quad (2.2)$$

Where,

$$[T_{\sigma}(\vartheta)] = \begin{bmatrix} m^2 & n^2 & 2mn \\ n^2 & m^2 & -2mn \\ -mn & mn & m^2 - n^2 \end{bmatrix}$$

and

$$[T_{\varepsilon}(\vartheta)] = \begin{bmatrix} m^2 & n^2 & mn \\ n^2 & m^2 & -mn \\ -2mn & 2mn & m^2 - n^2 \end{bmatrix}$$

It should be noted that [Q16] and [Q26] are zero but $[\bar{Q}_{16}]$ and $[\bar{Q}_{26}]$ are non zero except $\theta=0^{\circ}$ and 90° .

Now the stress-strain relationship in principle material direction is known. The reduced stiffness matrix [Q] in the global and local co-ordinate system is also known. So stress strain relationship for any layer in global coordinate system can be written as,

$$\begin{pmatrix} \sigma_x \\ \sigma_y \\ \tau_{xy} \end{pmatrix}_{kth} = [\bar{Q}_{x-y}]_{kth} [\varepsilon_{x-y}]_{kth} \quad (2.3)$$

2.2 Mid Plane Strain and Curvature of a Laminate

Since a Laminate contains multiple directions of laminae, it is convenient to choose a reference plane of the given Laminate. Then, structural behavior of the laminate can be referred to that of this plane. In lamination Theory the mid Plane of a laminate is chosen as the reference

plane.

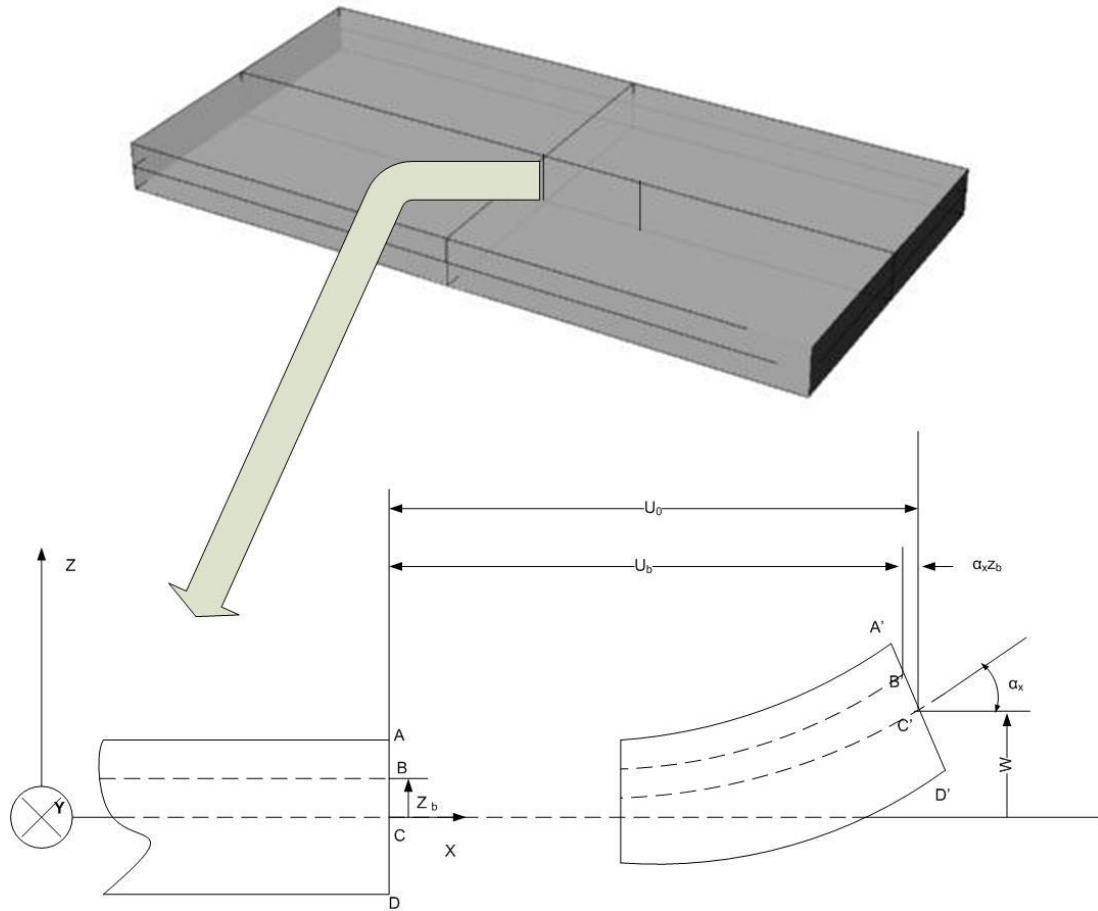


Figure 2.3 Laminated plate.

Let displacement functions of the mid plane of the laminated composite plate are $u_0 = u_0(x, y), v_0 = v_0(x, y), w_0 = w_0(x, y)$ as shown in the above figure 2.3. So the displacement of any point such as point B in the figure can be written as,

$$u = u_0 - \alpha_x z, v = v_0 - \alpha_y z, w = w_0$$

where

$$\alpha_x = \frac{\partial w}{\partial x}, \alpha_y = \frac{\partial w}{\partial y} \quad (2.4)$$

So stress at any point in the laminate can be obtained by,

$$\begin{aligned} \varepsilon_x &= \frac{\partial u}{\partial x} = \frac{\partial u_0}{\partial x} - z \frac{\partial^2 w}{\partial x^2} \\ \varepsilon_y &= \frac{\partial v}{\partial y} = \frac{\partial v_0}{\partial y} - z \frac{\partial^2 w}{\partial y^2} \\ \gamma_{xy} &= \frac{\partial u}{\partial y} + \frac{\partial v}{\partial x} = \frac{\partial u_0}{\partial y} + \frac{\partial v_0}{\partial x} - 2z \frac{\partial^2 w}{\partial x \partial y} \end{aligned} \quad (2.5)$$

Now we can define,

$$\begin{aligned} \varepsilon_0 &= \frac{\partial u_0}{\partial x} \\ \varepsilon_0 &= \frac{\partial v_0}{\partial y} \\ \gamma_{xy} &= \frac{\partial u_0}{\partial y} + \frac{\partial v_0}{\partial x} \end{aligned} \quad (2.6)$$

And,

$$\begin{aligned} \kappa_x &= z \frac{\partial^2 w}{\partial x^2} \\ \kappa_y &= -z \frac{\partial^2 w}{\partial y^2} \\ \kappa_{xy} &= -2z \frac{\partial^2 w}{\partial x \partial y} \end{aligned} \quad (2.7)$$

Equation 2.6 represents the mid plane strain and equation 2.7 represents the mid plane curvature. Combining equation 2.6 and equation 2.7 we can write in short,

$$\begin{bmatrix} \varepsilon_x \\ \varepsilon_y \\ \gamma_{xy} \end{bmatrix} = \begin{bmatrix} \varepsilon_x^0 \\ \varepsilon_y^0 \\ \gamma_{xy}^0 \end{bmatrix} + z \begin{bmatrix} \kappa_x \\ \kappa_y \\ \kappa_{xy} \end{bmatrix}$$

or

$$[\varepsilon_{x-y}] = [\varepsilon^0] + z [\kappa] \tag{2.8}$$

Equation 2.8 represents the strain of lamina at a distance z from the mid plane in terms of mid-plane strain and curvature. Substituting equation 2.8 into equation 2.3 we find,

$$\begin{pmatrix} \sigma_x \\ \sigma_y \\ \tau_{xy} \end{pmatrix}_{kth} = [\bar{Q}_{x-y}]_{kth} ([\varepsilon^0] + z_{kth} [\kappa]) \tag{2.9}$$

So, if we know the mid-plane strain and curvature and the distance of the layer from the mid-plane, then we can find the layer stress. Hence, the stress at any given layer can be obtained from the mid-plane strain and curvature of the laminate. The following section will discuss how to find the mid-plane strain and curvature from the applied load.

2.3 Constitutive Equation of a Laminate

The total forces and moments applied on the laminated plate is equal to the total internal forces and moments in the laminate. The following figure shows the definition of moments and loads in lamination theory. The resultant forces and moments per unit width of the laminate can be obtained by integrating the stresses of each ply through the thickness.

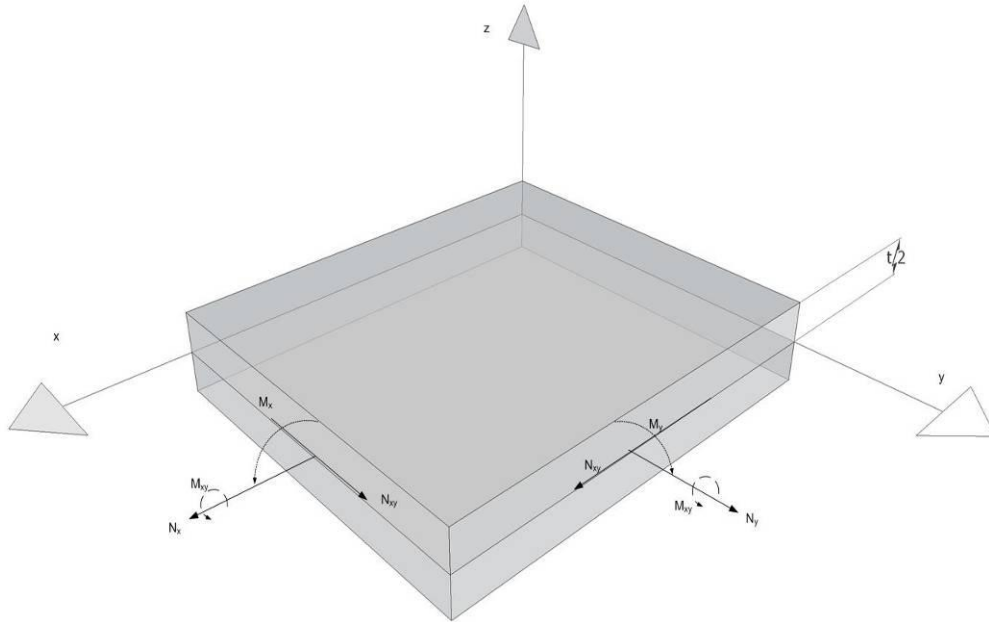


Figure 2.4 Loads and moments on a composite laminated plate.

The sum of forces and moments of each layer per unit width of laminate can be given by the following equations,

$$\begin{bmatrix} N_X \\ N_Y \\ N_{XY} \end{bmatrix} = \sum_{K=1}^n \int_{h_{k-1}}^{h_k} \begin{bmatrix} \sigma_x \\ \sigma_y \\ \tau_{xy} \end{bmatrix}_k dz \quad (2.10)$$

And,

$$\begin{bmatrix} M_X \\ M_Y \\ M_{XY} \end{bmatrix} = \sum_{K=1}^n \int_{h_{k-1}}^{h_k} \begin{bmatrix} \sigma_x \\ \sigma_y \\ \tau_{xy} \end{bmatrix}_k z dz \quad (2.11)$$

Substituting equation 2.9 in the above equations (2.10 and 2.11) we obtain,

$$[N] = [A][\varepsilon^0] + [B][\kappa]$$

where

$$[A] = \left\{ \sum_{k=1}^n \left[\bar{Q}_{X-Y} \right]_k (h_k - h_{k-1}) \right\} \quad (2.12)$$

$$[B] = \frac{1}{2} \sum_{k=1}^n \left[\bar{Q}_{X-Y} \right]_k (h_k^2 - h_{k-1}^2)$$

And,

$$[M] = [B][\varepsilon^0] + [D][\kappa]$$

where

$$[B] = \left\{ \frac{1}{2} \sum_{k=1}^n \left[\bar{Q}_{X-Y} \right]_k (h_k^2 - h_{k-1}^2) \right\} \quad (2.13)$$

$$[D] = \frac{1}{3} \sum_{k=1}^n \left[\bar{Q}_{X-Y} \right]_k (h_k^3 - h_{k-1}^3)$$

In the above equations, h_k and h_{k-1} are the coordinate of the k^{th} layer as illustrates in the following figure 2.5. From the figure it can be seen that the distance of each layer always calculated from the mid-plane. For an example if the k^{th} layer is considered then the distance is h_k which has been calculated from the mid-plane of the laminate. The [A], [B] and [D] matrix plays a vital role in stress analysis and predicting the behavior of composite. The [A] matrix is called the extensional stiffness matrix. [B] matrix is called the coupling stiffness matrix as it contributes in the coupling effect in response to different kind of load. [D] matrix is called the bending stiffness.

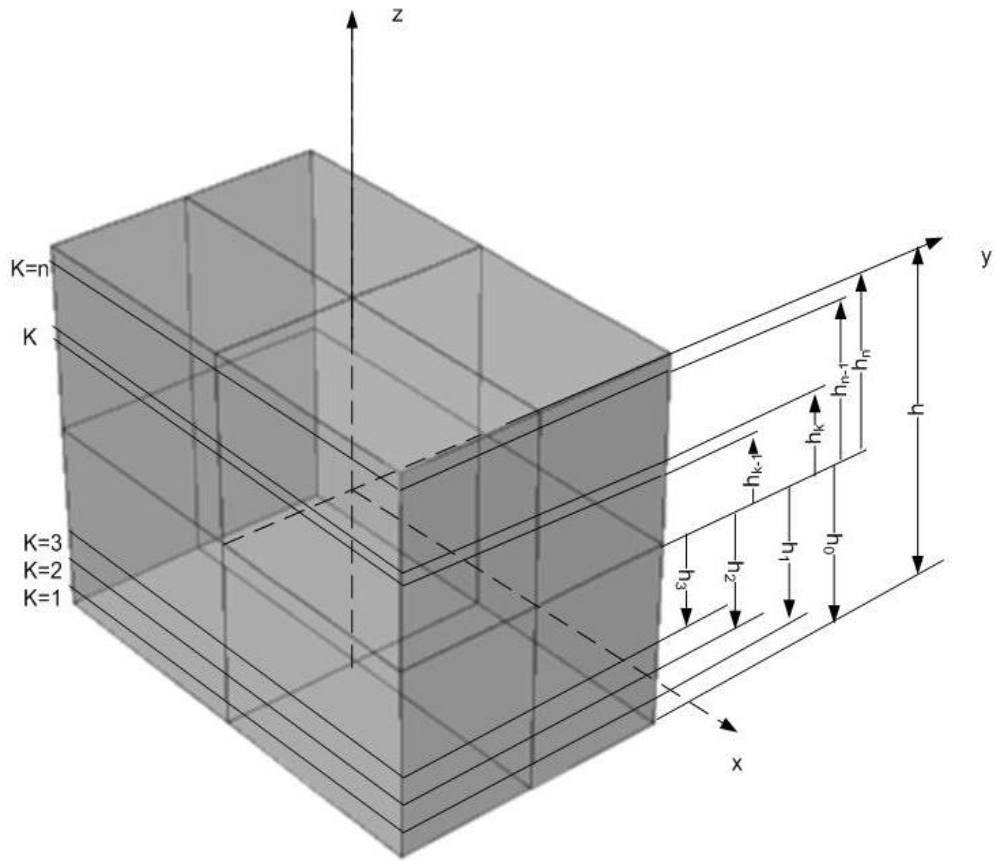


Figure 2.5 Layer orientation of a composite plate.

Combining equation 2.12 and equation 2.13 we get,

$$\begin{bmatrix} N \\ M \end{bmatrix} = \begin{bmatrix} A & B \\ B & D \end{bmatrix} \begin{bmatrix} \varepsilon^0 \\ \kappa \end{bmatrix} \quad (2.14)$$

From this equation mid-plane strain and curvature can easily be found. Putting those values in equation 2.5 stresses at any layer can be calculated. The structural characteristics of [A], [B] and [D] matrices have been extensively studied before [6].

2.4 Laminated beam theory of Rectangular Cross-section

All complicated structures are in fact collection and combination of simple structural members. Such a simple structural member is a flat beam. The foundation of the beam analysis is based upon the moment-curvature relationship along the longitudinal axis of the beam. This approach used for laminated composite beam is not different from the isotropic beam. However, in evaluation of the moment-curvature relationship, so-called the bending stiffness of the beam, laminated composite beam possesses a unique behavior that is different from the isotropic beam. This section will discuss on the axial and bending stiffness of the flat beam.

2.4.1 Axial Stiffness

The axial stiffness of a material means the resistance of that structure to deform along the loading direction. It is a proportional constant that relates the applied force and its strain response. From equation 2.14 we can write,

$$\begin{bmatrix} \varepsilon^0 \\ \kappa \end{bmatrix} = \begin{bmatrix} A & B \\ B & D \end{bmatrix}^{-1} \begin{bmatrix} N \\ M \end{bmatrix} \quad (2.23)$$

Or,

$$\begin{bmatrix} \varepsilon^0 \\ \kappa \end{bmatrix} = \begin{bmatrix} a & b \\ b^T & d \end{bmatrix} \begin{bmatrix} N \\ M \end{bmatrix} \quad (2.24)$$

From the compliance matrix shown in the above equation 2.24 assuming all the loads are zero ($N_y = N_{xy} = M_x = M_y = M_{xy} = 0$) and applying only N_x the first equation of the system becomes,

$$\varepsilon_x^0 = a_{11} \cdot N_x \quad (2.25)$$

$$\bar{N}_x = \left(\frac{w}{a_{11}} \right) \varepsilon_x^0 \quad (2.26)$$

$$\bar{A}_x = \left(\frac{w}{a_{11}} \right) \quad (2.27)$$

In composites, an equivalent Young's Modulus is equal to the inverse of a_{11} multiplied by the total height of the laminate. From equation 2.25

$$\varepsilon_x^0 = a_{11} \cdot N_x \rightarrow \frac{\tilde{\sigma}_x}{\varepsilon_x^0} = \frac{1}{a_{11}h} \rightarrow \tilde{E}_x = \frac{1}{a_{11}h} \quad (2.28)$$

where h is the thickness of the laminate and $\tilde{\sigma}_x$ is the average stress action on it.

Therefore, the axial stiffness can be written as,

$$\bar{A}_x = \tilde{E}_x A = \frac{w}{a_{11}} \quad (2.29 \text{ a})$$

2.4.2 Bending Stiffness

The bending stiffness of a material is defined as the resistance of that structure from bending. It is a proportional constant that relates the bending moment and its induced curvature.

It can be written as,

$$\bar{M}_x = \bar{D}_x \kappa_x$$

Applying analogous approach as equation 2.28 the bending stiffness can be written as,

$$\bar{D}_x^{smeared} = \tilde{E}_x I = \frac{1}{ha_{11}} I \quad (2.29 \text{ b})$$

2.5 Laminated Rectangular cross section beam considering stacking sequence

Beams are the primary structural members that carry bending loads. The axial stiffness and bending stiffness of composite beam depends on the deformation of the configuration of the

cross section. The configuration deformation is affected by the width of the beam. Hence in order to perform the analysis, narrow and wide beams need to be considered separately. Wide and narrow refer to the aspect ratio of the cross section that is the ratio of the cross section width to height. The following are a brief review of the work published in Ref. [7].

2.5.1 *Narrow Beam*

A narrow beam has a small width to height ratio. For a narrow beam the axial strain distribution give rise to deformation of the cross section in the transverse direction because of the poisson's ratio effect. For a narrow beam the load N_x and the moment M_x acting on the axial direction are only considered. The loads and the moments in the other directions are neglected.

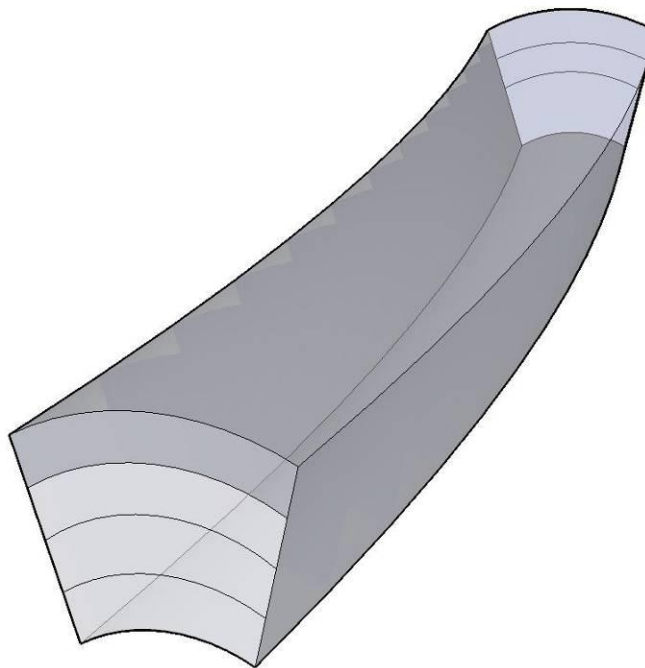


Figure 2.6 Narrow Beam

Substituting $N_y = N_{xy} = M_y = M_{xy} = 0$ in Equation 2.24 give the following equation,

$$\varepsilon_x^0 = a_{11}.N_x + b_{11}.M_x$$

$$\kappa_x = b_{11}.N_x + d_{11}.M_x$$

$$N_x = \frac{d_{11}}{a_{11}d_{11} - b_{11}^2}.\varepsilon_x^0 \quad (2.30)$$

$$M_x = \frac{a_{11}}{a_{11}d_{11} - b_{11}^2}.\kappa_x \quad (2.31)$$

From equation 2.30 the axial stiffness can be obtained since N_x is the axial force per unit width acting on the composite. Therefore substituting $N_x = \frac{\overline{N}_x}{w}$ in equation 2.30

we get axial stiffness,

$$\tilde{A}^{narrow}_x = \frac{wd_{11}}{a_{11}d_{11} - b_{11}^2} \quad (2.32)$$

Similarly from equation 2.31 we get,

$$\tilde{D}^{narrow}_x = \frac{wa_{11}}{a_{11}d_{11} - b_{11}^2} \quad (2.33)$$

There is a significance difference between the smeared property bending stiffness and the narrow beam bending stiffness. The smeared property approach bending stiffness does not account the stacking sequence in consideration. The smeared property approach considers only the equivalent Young's modulus and multiplied it with the inertia of the cross section, therefore the effect of stacking sequence on the bending stiffness is not taken into account. This ignorance is acceptable if the laminate is very thin and the distance of the ply location from the

reference axis of bending is relatively large. However, if the laminate is very thick and the distance from the bending axis very small, the stacking sequence will have a significant effect on the bending stiffness.

2.5.1 Wide Beam

Wide beam generally act like a Plate. It does not show distortion of the cross section like that of a narrow beam except for the outer edge. A wide beam is a beam which has a high width-height ratio as Shown in figure 2.6. As a result of this, curvature k_y and k_{xy} are restrained. It should be noted that the deformed configuration is intended to enhance the restrained effect of the beam cross-section.

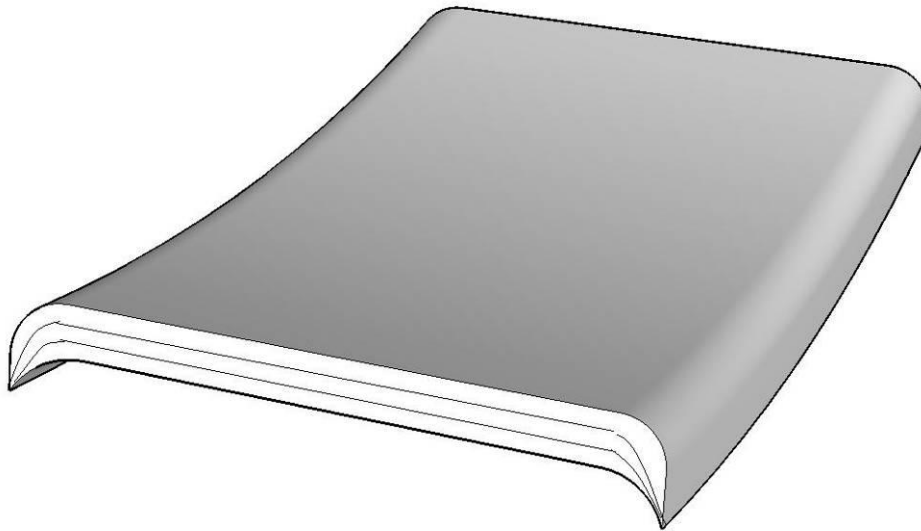


Figure 2.7 Wide Beam

Substituting $\boldsymbol{\varepsilon}_y^0 = \boldsymbol{\gamma}_{xy}^0 = \boldsymbol{\kappa}_y = \boldsymbol{\kappa}_{xy} = \mathbf{0}$ in Equation 2.14 gives the

following equations,

$$N_x = A_{11} \cdot \varepsilon_x^0 + B_{11} \cdot \kappa_x$$

$$M_x = B_{11} \cdot \varepsilon_x^0 + D_{11} \cdot \kappa_x$$

Writing these Equations in matrix form we get,

$$\begin{bmatrix} \varepsilon_x^0 \\ \kappa_x \end{bmatrix} = \begin{bmatrix} A_{11} & B_{11} \\ B_{11} & D_{11} \end{bmatrix}^{-1} \begin{bmatrix} N_x \\ M_x \end{bmatrix} \text{ and } \begin{bmatrix} N_x \\ M_x \end{bmatrix} = \begin{bmatrix} A_{11} & B_{11} \\ B_{11} & D_{11} \end{bmatrix} \begin{bmatrix} \varepsilon_x^0 \\ \kappa_x \end{bmatrix}$$

$$\varepsilon_x^0 = \frac{D_{11}}{A_{11}D_{11} - B_{11}^2} \cdot N_x \quad (2.34)$$

$$\kappa_x = \frac{A_{11}}{A_{11}D_{11} - B_{11}^2} \cdot M_x \quad (2.35)$$

Rearranging Equation 2.34, it is possible to relate the axial force per unit width and the axial strain,

$$N_x = \left(A_{11} - \frac{B_{11}^2}{D_{11}} \right) \cdot \varepsilon_x^0 \quad (2.36)$$

Substituting $N_x = \frac{\bar{N}_x}{w}$ in equation 2.36 we find,

$$\bar{A}_x^{wide} = w \left(A_{11} - \frac{B_{11}^2}{D_{11}} \right) \quad (2.37)$$

Rearranging Equation 2.35 we get,

$$\bar{D}_x^{wide} = w \left(D_{11} - \frac{B_{11}^2}{A_{11}} \right) \quad (2.38)$$

Where, w is the width of the laminate.

2.6 Laminated beam theory with curved cross section

The following is a brief review of constitutive equations of a laminated curved beam which is derived by Nyugen [8].

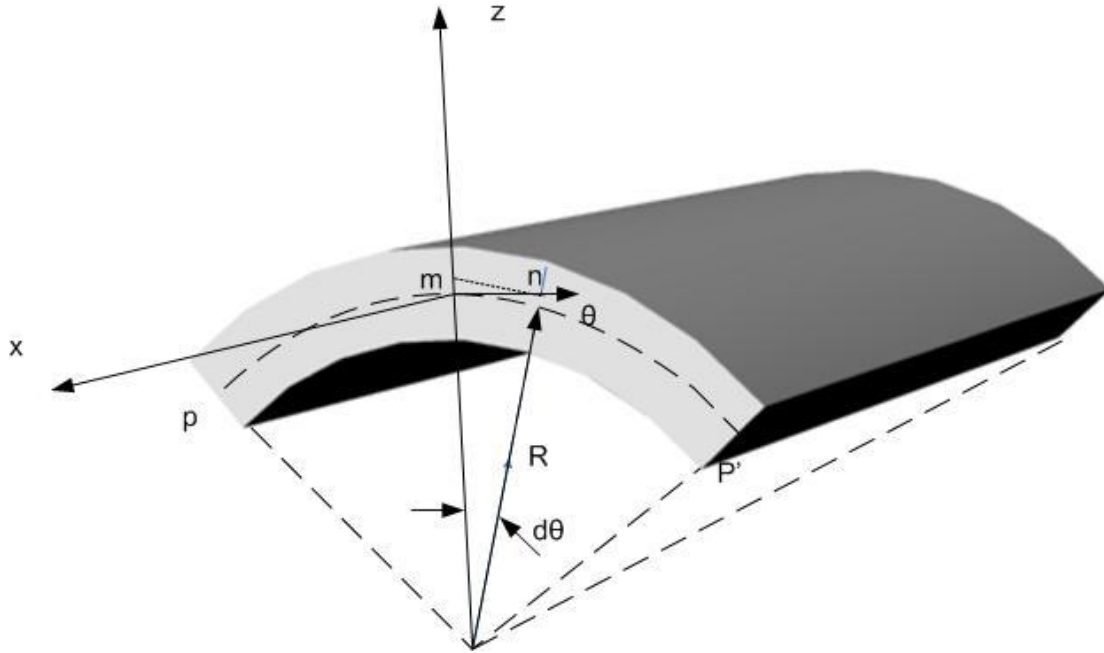


Figure 2.8 Curved Beam.

Let pp' be the mid axis of the beam. The differential element at k^{th} layer from the mid axis is \overline{mn} . Then the elongation after deformation can be written as

$$(R+z)d\theta \cdot \varepsilon_{\theta} \quad (2.15)$$

The deformation can also be described in terms of the mid-plane strain ε_{θ} and their curvature κ ,

$$R \cdot d\theta (\varepsilon_{\theta} + z \cdot \kappa) \quad (2.16)$$

Combining equation 2.15 and 2.16,

$$\varepsilon_{\theta} = \frac{R}{R+z} (\varepsilon_0 + z \cdot \kappa) \quad (2.17)$$

For simplicity, the stress σ_{θ} at kth layer can be approximated by,

$$\sigma_{\theta,k} = \bar{Q}_{\theta\theta,k} \varepsilon_{\theta,k} \quad (2.18)$$

The resultant force and moment per unit width, N_{θ} and M_{θ} are obtained as,

$$\begin{aligned} N_{\theta} &= A_{\theta\theta} \varepsilon_0 + B_{\theta\theta} \kappa \\ M_{\theta} &= B_{\theta\theta} \varepsilon_0 + D_{\theta\theta} \kappa \end{aligned}$$

where,

$$\begin{aligned} A_{\theta\theta} &= \sum_{k=1}^n \bar{Q}_{\theta\theta,k} \int_{z_{k-1}}^{z_k} \frac{R dz}{R+z} \\ B_{\theta\theta} &= \sum_{k=1}^n \bar{Q}_{\theta\theta,k} \int_{z_{k-1}}^{z_k} \frac{Rz dz}{R+z} \\ D_{\theta\theta} &= \sum_{k=1}^n \bar{Q}_{\theta\theta,k} \int_{z_{k-1}}^{z_k} \frac{Rz^2 dz}{R+z} \end{aligned} \quad (2.19)$$

Explicitly,

$$\begin{aligned} A_{\theta\theta} &= R \sum_{k=1}^n \bar{Q}_{\theta\theta,k} \ln \frac{R+z_k}{R+z_{k-1}} \\ B_{\theta\theta} &= R \sum_{k=1}^n \bar{Q}_{\theta\theta,k} \left[(z_k - z_{k-1}) - R \ln \frac{R+z_k}{R+z_{k-1}} \right] \\ D_{\theta\theta} &= R \sum_{k=1}^n \bar{Q}_{\theta\theta,k} \left[\frac{1}{2} (z_k^2 - z_{k-1}^2) - R(z_k - z_{k-1}) - R^2 \ln \frac{R+z_k}{R+z_{k-1}} \right] \end{aligned} \quad (2.20)$$

Combining the equations,

$$\begin{bmatrix} N_{\theta\theta} \\ M_{\theta\theta} \end{bmatrix} = \begin{bmatrix} A_{\theta\theta} & B_{\theta\theta} \\ B_{\theta\theta} & D_{\theta\theta} \end{bmatrix} \begin{bmatrix} \varepsilon^0 \\ \kappa_\theta \end{bmatrix} \quad (2.21)$$

Or,

$$\begin{bmatrix} \varepsilon^0 \\ \kappa_\theta \end{bmatrix} = \begin{bmatrix} A_{\theta\theta} & B_{\theta\theta} \\ B_{\theta\theta} & D_{\theta\theta} \end{bmatrix}^{-1} \begin{bmatrix} N_{\theta\theta} \\ M_{\theta\theta} \end{bmatrix} \quad (2.22)$$

Where, $A_{\theta\theta}$, $B_{\theta\theta}$, $D_{\theta\theta}$ are extensional, coupling and bending stiffness along the θ direction respectively.

CHAPTER 3

FINITE ELEMENT MESHING

The accuracy of finite element solution depends on the choice of the mesh. If the selected mesh violates the symmetry of the problem, the resulting solution will be less accurate than one aligned with the symmetry of the problem. This is called the effect of geometrical isotropy. Triangular mesh can be used for analysis because of their complete polynomial representation to the corresponding order and their flexibility in representation of geometric complexity. However, it has been known that geometrical anisotropy arises with this element. Reddy [9] pointed out that triangular element has fewer lines of symmetry when compared with rectangular element. This effect may be more significant for application of laminated structures. Chan and Chen [10] has shown the effect of Geometric Isotropy on a [0/90]_s laminate under uniformly distributed load. 2D layered elements were used for their study. The effect of this geometric isotropy can be reduced if higher number of element is used or higher order element is used. Here a Symmetric layup of [$\pm 45/0/90$]_s under tension case were tested. Three different kind of mesh with approximately same element number and same boundary conditions were used and compared with closed form solution. The closed form equations are stated below.

$$\begin{aligned} u(x, y) &= \left(a_{11}x + \frac{a_{16}}{2}y \right) N_x \\ v(x, y) &= \left(\frac{a_{16}}{2}x + a_{12}y \right) N_x \end{aligned} \quad (3.1)$$

The following figure will show the Type of mesh that has been used for this analysis. Point to be noted that the figure a with a quad mesh satisfy the criteria of geometric isotropy, Figure b with a free triangular mesh partially satisfy the geometric isotropy and figure c with

triangular mapped mesh does not satisfy the geometric isotropy at all, because the models symmetry line is parallel to the diagonal line connecting point 2 and 4.

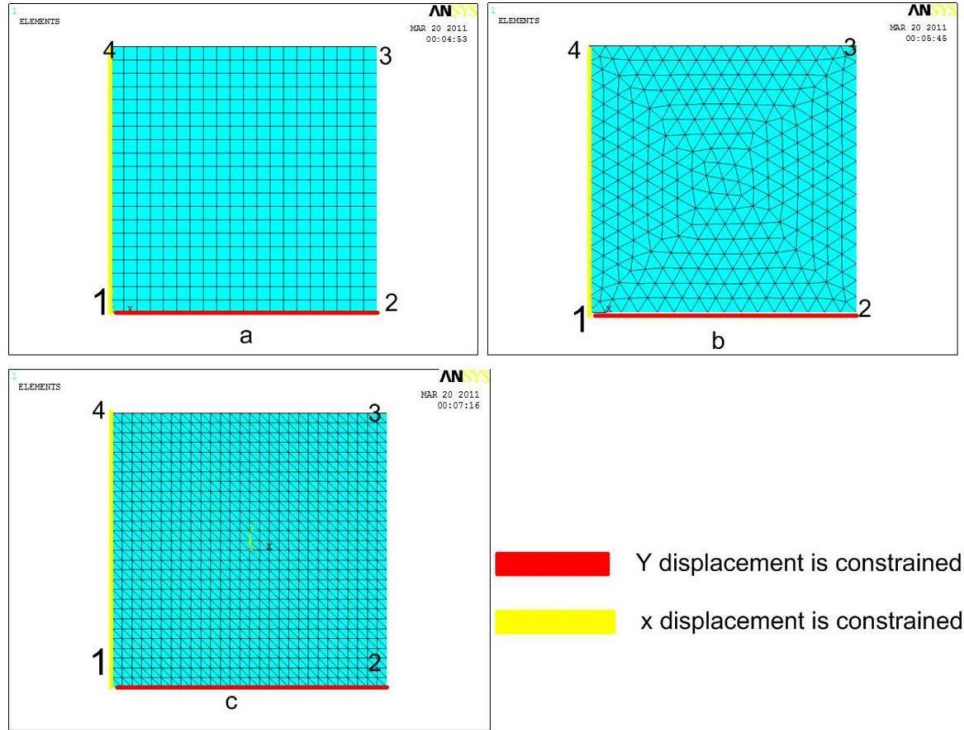


Figure 3.1 Different kind of mesh

The geometry of all the models in above figure 3.1 is 0.25*0.25 inch². The displacement results at point 3 have been tabulated in the flowing table.

Table 3.1 Results for a 3D Plate with Different Mesh Type

10^{-4}	Mesh a	Mesh b	Mesh c	Closed-form equation result
u	0.29441	0.29441	0.29441	0.29441
v	-0.088258	-0.088258	0.088258	-0.088258

From the above analysis much difference is not observed because the number of element taken was sufficient. More over a shell 99 element with 8 node and after degenerated 6

node was used. Chen [8] has show that for a constant strain triangular element the effect of geometric isotropy plays a vital role.

In finite element analyses meshing always plays a great roll. It's been always a difficult question for designers to answer that –what will be the appropriate mesh size. Actually there is no definite answer to that question. In case of composite the care that should be taken during modeling is even more. The criteria that should be considered while modeling a composite can be summarized as follows,

- Choosing proper mesh size: the mesh should not be so fine that it becomes very expensive to run on the other hand it should not be so coarse that the result of the solution comes incorrect.
- Aspect ratio is very important while doing the 3d composite model
- Special care should be taken while doing meshing where there is a geometrical discontinuity.

3.1 Choosing proper mesh size

To describe the effect of mesh size on finite element solution we take a simple plate with a hole and meshed it with mapped mesh. The SHELL99 layer element of ANSYS was used to model a symmetric layup of $[\pm 45/0/90]_s$ with a hole.. Results were taken for far field and maximum stress in each layer. Mesh 1 is the coarsest mesh and mesh 3 is the finest mesh. A comparison of the lamination theory is also given. In these models, the mesh with geometrical isotropy was maintained.

To create the mesh, the area near the circular cut out was subdivided into smaller areas. And a line set attribute was selected per line. All the areas were glued together to create the whole geometry. The composite plate geometry is 5 inches by 2 inches. The following figure will show the meshing technique for mesh near the cut-out section

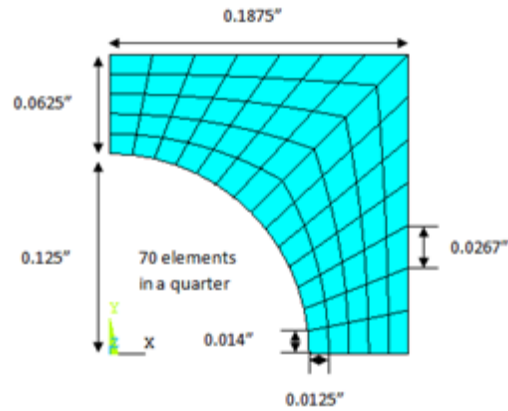
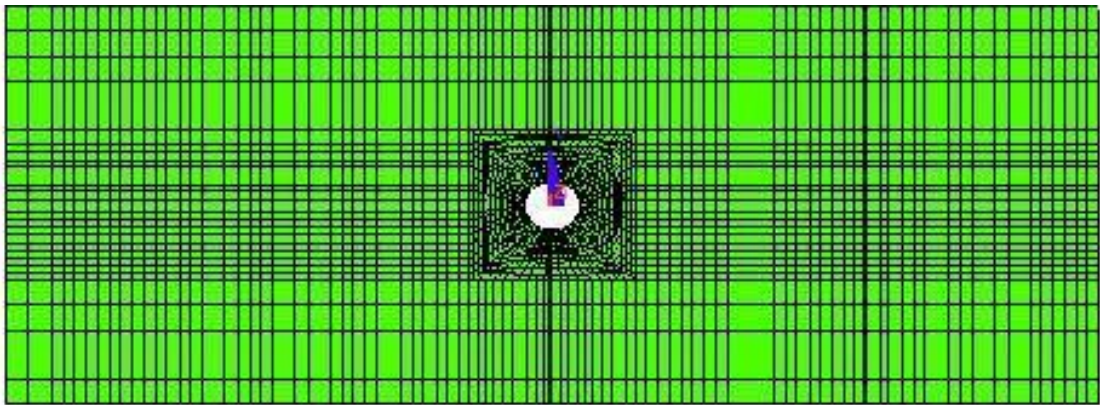
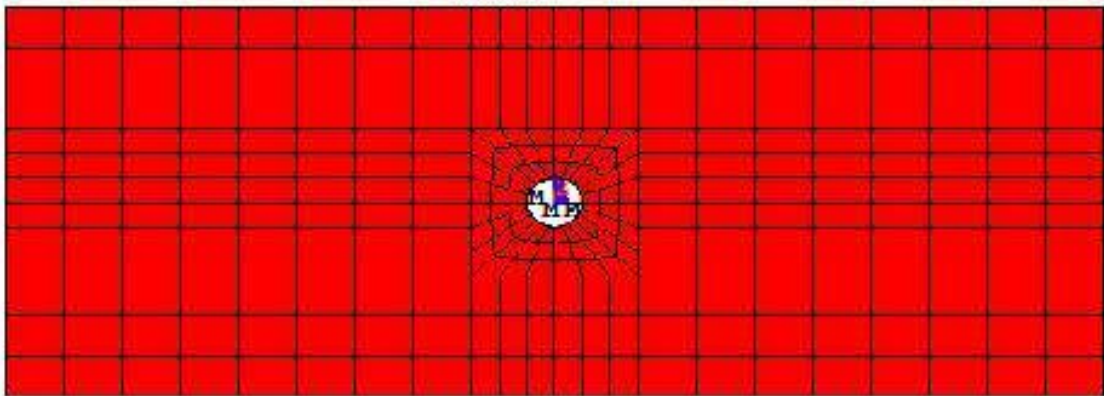


Figure 3.2 Circular cut-out.

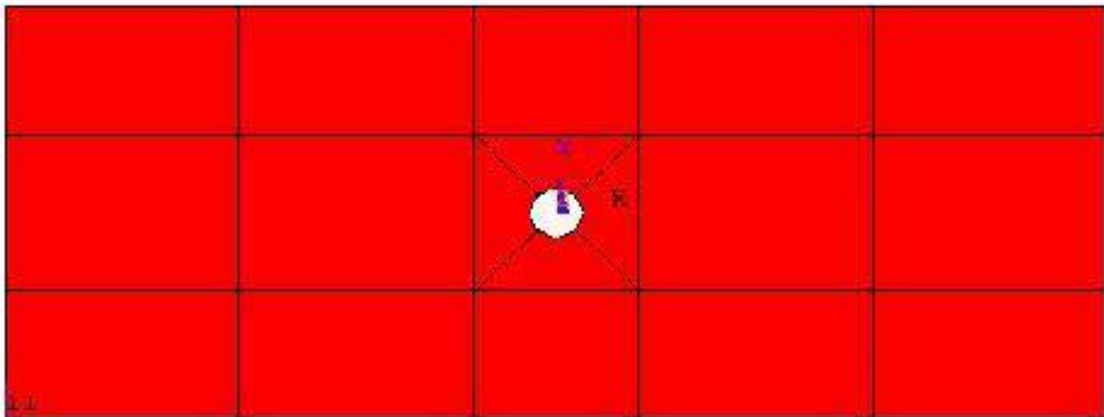
The next figure (3.3) will show the meshes that have been used in these analyses. The meshes were created by mapped meshing. Mesh 1 has the lowest number of elements. Mesh 2 has higher element number than Mesh 1, and mesh 3 has the highest element numbers. Same boundary conditions were applied for the three dimensional models. Symmetric lay-up of $[\pm 45/0/90]_s$ were used for this analysis. The laminate with a symmetric and balanced layup gives no shear coupling and no bending/twisting effect. Stress results were taken away from the hole because the objective was not to capture the stresses at the close vicinity of the hole, rather to see the effect at a point away from the hole in presence of a discontinuity in the model. The results are listed below in Table 3.2.



Mesh3



Mesh2



Mesh1

Figure 3.3 Different Mesh size.

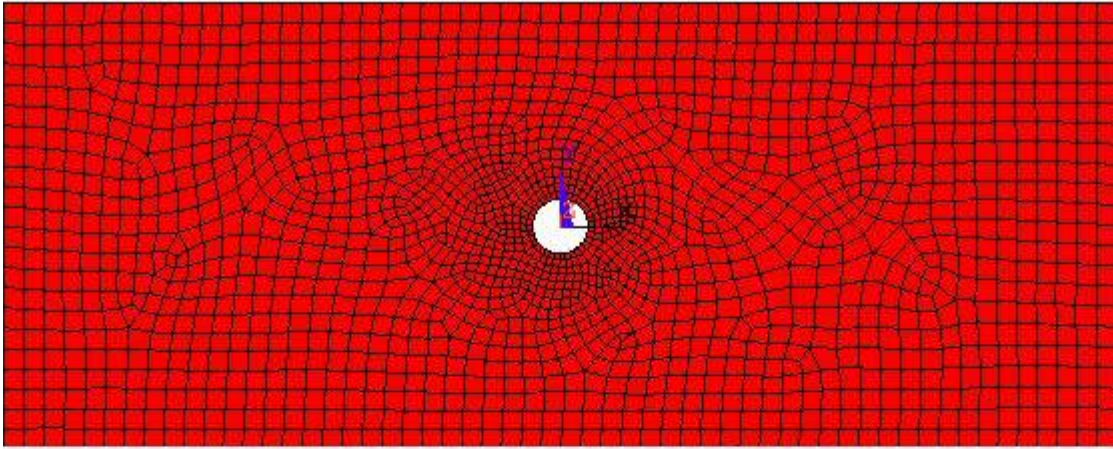
Table 3.2 Mesh size results for a 2D Plate with a hole

2D full model of layup [$\pm 45/0/90$]s results using shell 99 element												
	Mesh 1			Mesh2			Mesh 3			CLT (Base Line)		
	σ_x	σ_y	τ_{xy}	σ_x	σ_y	τ_{xy}	σ_x	σ_y	τ_{xy}	σ_x	σ_y	τ_{xy}
45	638	367	420	630	368	416	633	366	417	633	366	417
-45	638	367	-420	630	368	-416	633	366	-417	633	366	-417
0	2591	-10	0	2522	-8	0	2559	-9	0	2559	-9	0
90	177	-745	0	172	-690	0	174	-724	0	174	-724	0
90	177	-745	0	172	-690	0	174	-724	0	174	-724	0
0	2591	-10.3	0	2522	-8	0	2559	-9.4	0	2559	-9.4	0
-45	638	367	-420	630	368	-416	633	366	-417	633	366	-417
45	638	367	420	630	368	416	633	366	417	633	366	417

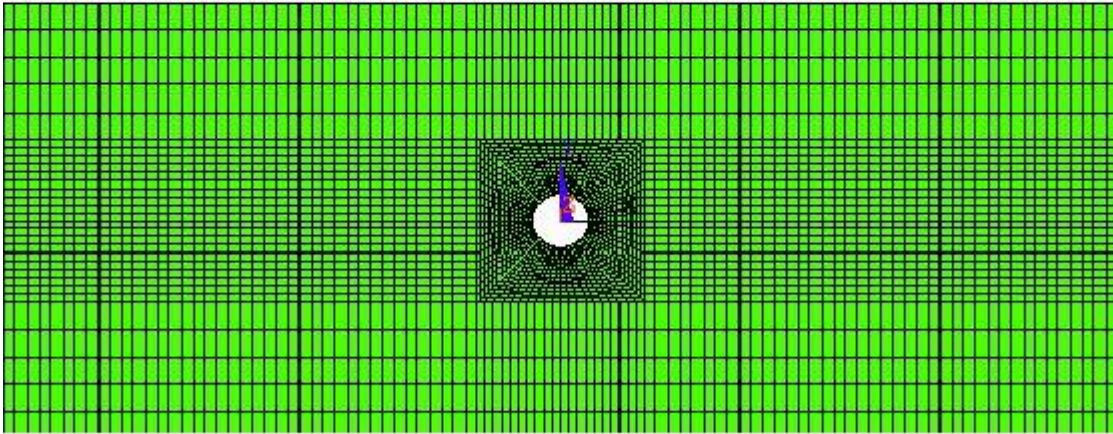
From the table it is clearly seen that the stress results obtained from the three quite different meshes give insignificant difference for the stress at the location away from the hole region.

3.2 Auto mesh

Mapped mesh is always preferred while doing a composite model, because it agrees with the geometrical symmetry of the material. Here an example is sited to compare a mapped mesh with a free mesh. Quad element of Shell 99 is used again for these analyses. Total no of element for the free mesh was 1715 and mapped mesh was 2050.



Free mesh



Mapped mesh

Figure 3.4 Free versus Mapped mesh.

Table 3.3 Free versus mapped Mesh for a 2D Plate with a hole

	Free Mesh			Mapped Mesh			CLT (Base Line)		
	σ_x	σ_y	τ_{xy}	σ_x	σ_y	τ_{xy}	σ_x	σ_y	τ_{xy}
45	627.5	367	414	633	366	417	633	366	417
-45	630.5	370	-418	633	366	-417	633	366	-417
0	2520	-7.5	-0.2	2559	-9	0	2559	-9	0
90	172.3	-690	-0.2	174	-724	0	174	-724	0
90	172.3	-690	-0.2	174	-724	0	174	-724	0
0	2520	-7.5	-0.2	2559	-9.4	0	2559	-9.4	0
-45	630.5	370	-418	633	366	-417	633	366	-417
45	627.5	367	414	633	366	417	633	366	417

From the table it is clear that the mapped mesh gives better results compared with the results by classical lamination theory. This is because in mapped mesh geometrical symmetry of the model is preserved.

3.3 Aspect ratio

Aspect ratio of finite element is another important issue that has to be considered while modeling composite structure. By nature composite layers are very thin. Hence, it is not practical to keep a small aspect ratio in modeling a composite laminate because of limited computer capacity. The aspect ratio is defined as..

$$\text{Aspect Ratio} = \frac{\ell}{t_{\text{ply}}} \quad (3.2)$$

Where, ℓ and t_{ply} are defined in figure 3.5. ℓ is the larger dimension on the laminate

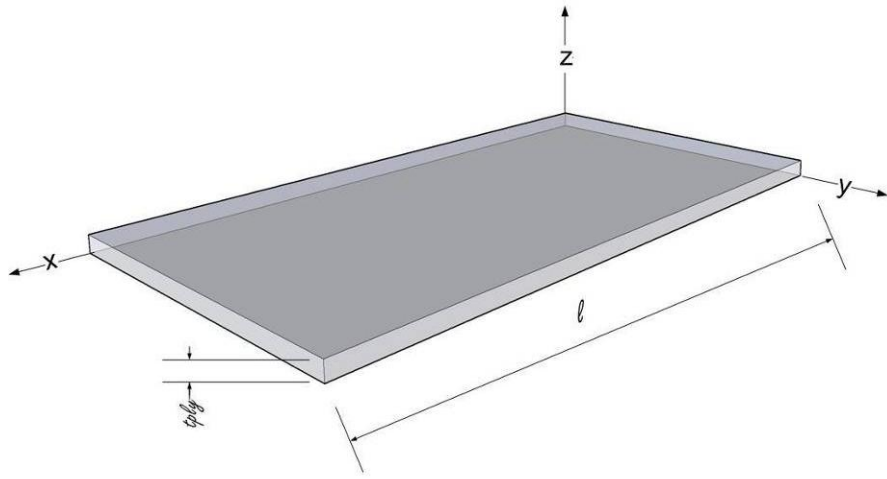


Figure 3.5 Aspect Ratio

To investigate the stress effect due to the aspect ratio of finite element, a symmetric lay-up of $[\pm 45/0/90]_s$ was used for this analysis. Table 3.4 lists ply stresses obtained from the model with different aspect ratio. The aspect ratio has been calculated from the equation 3.2. It can be easily observed from the table that the results converges with the lower aspect ratio. It should be noted that unlike aspect ratio of 5, the stress of +45 and - 45 plies for aspect ratio, 25 are not identical. This is because only four elements were allowed in the model. Hence, the stresses are strongly influenced by the presence of the edge stress.

Table 3.4 Aspect Ratio Results for a Flat Plate

	Aspect Ratio = $\frac{\ell}{\text{tply}} = 25$			Aspect Ratio = $\frac{\ell}{\text{tply}} = 17$			Aspect Ratio = $\frac{\ell}{\text{tply}} = 10$			Aspect Ratio = $\frac{\ell}{\text{tply}} = 5$		
	σ_x	σ_y	τ_{xy}	σ_x	σ_y	τ_{xy}	σ_x	σ_y	τ_{xy}	σ_x	σ_y	τ_{xy}
45	606	356	409	620	369	438	640	375	428	634	362	418
-45	522	302	-351	613	352	-401	634	368	-418	634	368	-418
0	2670	-13.71	-1.38	2593	-6	-3	2545	-9	-1	2562	-11	0
90	171.23	-759	0	135	-709	0.4	174	-728	0.8	174	-719	0.8
90	171.23	-737	0	135	-727	0.4	166	-729	0.2	174	-719	1.3
0	2670	-13.71	0	2556	-9	0.4	2585	-7	0.9	2562	-11	0
-45	686.4	412	-462	666	399	-447	634	367	-418	634	368	-418
45	606	332	403	627	366	413	622	356	407	634	362	418

CHAPTER 4

ONE-DIMENSIONAL, TWO DIMENSIONAL, THREE-DIMENSIONAL MODELINGS

A structure can be divided into elements which can be one dimensional (beam), two dimensional (plate) or three dimensional (brick) elements. These types of elements are often selected based upon the preferred structural configuration and its interested structural response. Generally in finite element, if the one dimension of the model is ten times greater than the other shell element should be chose instead of solid and if two dimension of the model is ten times greater than the other beam element should be preferred. But because of the anisotropic nature of composite mostly composites are modeled by two dimensional element containing all the layers and occasionally in three dimension by stacking a 3D element of each layer through the thickness.

Since composite layers are very thin, using a 3D model for a composite structure requires a large computing capacity because of the aspect ratio requirement of 3D elements. On the other hand using a 2D model requires smearing of laminate properties. As a result inter laminar response will be ignored. Hence selection of a 2D or a 3D element depends on whether the response of the inter-laminar behavior is needed. A brief discussion on Elements that can be used for composite modeling is given below.

Shell elements can be imagined as collapsed solid elements, which have negligible through thickness stress values. Since some edges are absent in shell elements, generally more degrees of freedom (rotational degrees of freedom) are defined for nodes of a shell element. For some specific applications, instead of solid elements SHELL99 can be used depending on geometrical considerations. SHELL 91 is used with nonlinear applications such as large strain, sandwich construction or plasticity. SHELL181 is a 4-node element. It is not always preferred in composite modeling since highly nonlinear behavior exists. In using

SHELL99, layered configuration can be modeled by specifying the layer properties such as material properties, orientation angle, layer thickness and number of integration points per layer.

Table 4.1 Elements with composite capability in Ansys

Elements	Description
SHELL 99	Linear Layered Structural Shell Element
SHELL 91	Nonlinear Layered Structural Shell Element
SHELL 181	Finite Strain Shell
SHELL 281	Finite Strain Shell
SOLSH190	3D Layered Structural Solid
SOLID 46	3-D Layered Structural Solid Element
SOLID 185	3-D Layered Structural Solid Element
SOLID 186	3-D Layered Structural Solid Element
SOLID 191	Layered version of SOLID 95
SOLID 95	Has composite capabilities
SHELL 63	Can be used for composite
SOLID 65	3D reinforced concrete solid element
BEAM 188	Finite strain Beam
BEAM 189	Finite strain Beam

For SOLID 46 and SHELL 99 element types of ANSYS, constitutive matrices can be defined with an 'infinite number of layers' opportunity. Within layered configuration, SHELL 63, SHELL 91, SHELL 181 and SHELL 63 elements of ANSYS permit sandwich construction using one layer and real constants. It is possible to model ply drop-off, by using SHELL 181, SHELL 91 and SHELL 99 elements, by the method of node offsetting. Shell 99 is an eight node Linear

Layered Structural Shell Element, which can be used to model composite structures up to 250 layers. Beyond this value, using a user-input constitutive matrix, more than 250 layers can be modeled. It does not support some nonlinear properties that SHELL 91 supports, but it has smaller computational time. Shell 99 has eight nodes: four corner nodes and four mid side nodes. Each node has six degrees of freedom: translations in three directions and rotation about three axes. An average or each corner thickness can be defined explicitly, which gives a bi-linearly varying thickness over the area of the layer, with the thickness input at the corner node locations. Inter laminar shear stresses can be calculated. Elastic properties, layer orientation and density are the user-defined material properties. Stress stiffening and large deflections are supported. The element coordinate system for Shell99 is right handed. Positive x-axis of the element coordinate system is defined by the direction from 'node I' to 'node J' (Figure 4.1) of the each element. The first layer is defined as the bottom layer, on negative z direction. Angle of fiber orientation is defined as the angle from x-axis to a direction, rotated toward y-axis of element coordinate system.

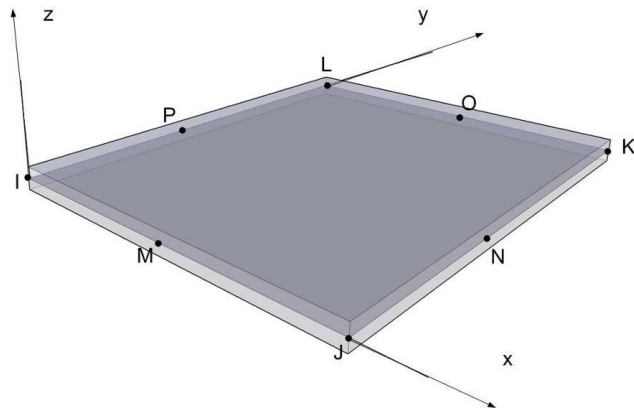


Figure 4.1 Shell 99 Element Coordinate system

In this study, SHELL99 was selected for two-dimensional model, SOLID186, for three-

dimensional model and BEAM188 for one dimensional modeling. SOLID186 can be used in both layered and non-layered options. Non-layered option was used here. The beam elements are based on Timoshenko beam theory, which is a first order shear deformation theory: transverse shear strain is constant through the cross-section; that is, cross-sections remain plane and undistorted after deformation. BEAM188 allows change in cross-sectional inertia properties as a function of axial elongation. By default, the cross-sectional area changes such that the volume of the element is preserved after deformation. BEAM188 does not account for coupling of bending and twisting at the section stiffness level. The transverse shears are also treated in an uncoupled manner. This may have a significant effect on layered composite and sandwich beams if the layup is unbalanced. The beam elements are based on Timoshenko beam theory which is a first order shear deformation theory- Transverse shear strain is constant through the cross section, which means cross-section remains plane and undistorted after deformation.

A composite layer requires four basic material constants to fully describe its structural behavior, namely modulus of elasticity in fiber direction E_1 , modulus of elasticity transverse to the fiber direction E_2 , in- plane shear modulus G_{12} , and in-plane poisson ratio ν_{12} . There are generally two ways to supply these material data to FEM software such as ANSYS. Moduli of the lamina or laminate stiffness are two typical inputs as material data.

The one-dimensional beam requires the modulus of composite layer along the axis of the beam. However, a composite layer is inherent two-dimensional properties. Hence, the equivalent modulus for the beam element is often used.

For a layered element, SHELL99, the input of the material constants can be either in matrix form or layer form by using KEYOPT(2). For the input in matrix form, the matrices, A, B, D must be computed outside of the ANSYS program or from a prior ANSYS run using KEYOPT(10). In the layer input of the material constants, the layer fiber orientation and

stacking sequence are directly input in the software for most common FEM codes. The code will then calculate the equivalent material constants for the entire laminate by using classical lamination theory.

In modeling thick composite structures, 3D elements are usually preferred because the geometry of such structure is more solid than plate like. However for a thin laminate, three dimensional state of stress exists in the neighborhood of free edge such as a cutout edge and near the edge of the laminate. In this case a 3D model must be used.

The detailed modeling techniques of 1D, 2D and 3D models used in this thesis has been described in Appendix A.

4.1 One Dimensional Modeling

Using one-dimensional model for a composite structure, the equivalent properties are calculated and incorporate them as a one dimensional element. The conventional method of doing that is by following equations:

$$\begin{aligned}
 \overline{E}_x &= \frac{1}{a_{11}t} \\
 \overline{E}_y &= \frac{1}{a_{22}t} \\
 \overline{G}_{xy} &= \frac{1}{a_{66}t} \\
 \overline{\nu}_{xy} &= -\frac{a_{21}}{a_{11}}
 \end{aligned}
 \tag{4.1}$$

Where a_{11} , a_{12} , a_{22} , a_{66} and t are the compliance components and thickness of laminate used for SHELL99. Chen and Chan [10] found that using the calculated equivalent properties obtained by this conventional method in finite element modeling results in a significant error in the ply stress prediction for laminate with an unsymmetrical and unbalanced layup but insignificant error for symmetric and balanced laminate. Their suggested equations for

equivalent properties for a general laminate [10] are listed as follows,

$$\begin{aligned}
 E_x &= \frac{1}{\left(P_{11} - \frac{P_{16}^2}{P_{66}}\right)t} \\
 E_y &= \frac{1}{\left(P_{22} - \frac{P_{26}^2}{P_{66}}\right)t} \\
 \nu_{xy} &= -\frac{P_{12} - \frac{P_{16}P_{26}}{P_{66}}}{P_{11} - \frac{P_{16}^2}{P_{66}}} \\
 G_{xy} &= \frac{1}{\left[P_{66} - \frac{1}{\Delta_1} \left(P_{16}^2 P_{22} - 2P_{12}P_{26}P_{16} + P_{26}^2 P_{11}\right)\right]t} \\
 \text{where,} \\
 [P] &= [a] - [b][d]^{-1}[b^T] \\
 \Delta_1 &= P_{11}P_{22} - P_{12}^2
 \end{aligned} \tag{4.2}$$

An example of a simple supported beam with a symmetric layup of $[\pm 45/0/90]_s$ and a unsymmetrical layup of $[\pm 45/0/90]_{2T}$ is used to study the maximum beam deflection by using two different methods of equivalent property in the finite element model. Figure 4.2 illustrates the geometry and the loading condition of the beam. Both conventional and modified methods of calculating equivalent properties have been used in the ANSYS analysis. The results of the deflection were compared with the closed form solution shown in equation 4.3.

$$\nu_{\max} = \frac{PL^3}{48.D_x} \tag{4.3}$$

Where, the bending rigidity D_x was calculated by the method shown in equation 2.38.

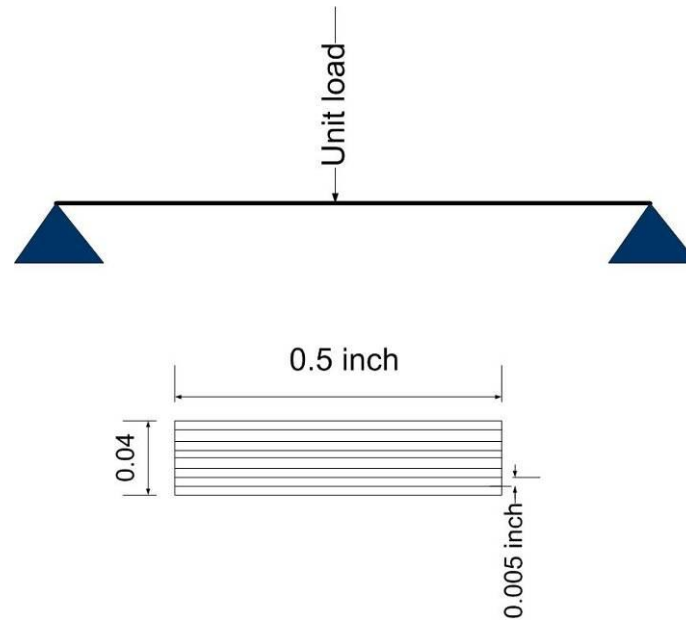


Figure 4.2 Simply Supported Beam.

The composite material properties used for this analysis is shown below, this material property has been used for all the models in this thesis.

Table 4.2 Material properties used in this Study

<i>Properties</i>	<i>value</i>
<i>E11</i>	<i>21.75 msi</i>
<i>E22=E33</i>	<i>1.595 msi</i>
<i>v12=v13, v23</i>	<i>0.25,0.45</i>
<i>G12=G13 , G23</i>	<i>0.8702 msi, 0.5366 msi</i>
<i>t</i>	<i>0.005 inch</i>

The equivalent properties of the laminates calculated by two methods are listed in Table 4.3. As indicated, two methods give exactly the same results for the symmetric and balanced

laminate, but a significantly different result for unsymmetrical and balanced laminate.

Table 4.3 Equivalent modulus

Equivalent properties		Ex Msi	Ey Msi	vxy	Gxy Msi
[±45/0/90] _s	conventional	8.4915	8.4915	0.2998	3.2665
	Modified	8.4915	8.4915	0.2998	3.2665
[±45/0/90] _T	Conventional	8.0859	7.4745	0.3508	2.905
	Modified	8.4915	8.4915	0.2998	3.2665

The following table shows the maximum deflection of the beam results obtained from FEM solution. The results have been compared with a closed form solution. As the FEM model is one dimensional the equivalent properties from the above table has been used to define the material properties.

Table 4.4 Conventional method versus Modified method 1D FEM beam deflection

	equivalent properties by conventional method		equivalent properties by modified method		Closed form solution	
	Symmetric, Balanced [±45/0/90] _s	Un-symmetric, Balanced [±45/0/90] _T	Symmetric, Balanced [±45/0/90] _s	Un-symmetric, Balanced [±45/0/90] _T	Symmetric, Balanced [±45/0/90] _s	Un-symmetric, balanced [±45/0/90] _T
Laminate stacking sequence						
displacement	0.024875	0.026118	0.024875	0.024875	0.02490	0.02510

It can be seen from table above that for a symmetric laminate the conventional and the modified method both agree with the closed form solution, but for an Un-balanced laminate the

conventional method does not agree with closed form solution.

4.2 Two and Three Dimensional Modeling

For an isotropic plate, a full, a half or even a quarter model are selected for two dimensional analysis by taking advantage of symmetry condition of loading and geometry of the structure. No matter what type of modeling was used, the result agrees well among all of the models. However, this may not be true for modeling a composite structure. To address this issue, the symmetric layup of $[\pm 45/0/90]_s$ and an un-symmetric layup of $[\pm 45/0/90]_{2T}$ were used in this study.

Material properties are same as indicated in Table 4.1. The following table will show the geometric of the models.

Table 4.5 Geometry of 2D full model and 2D quarter model

Geometry in inch	2D full model	2D quarter model
Plate without hole	0.5*0.5	0.25*0.25

A simple tension load has been applied to the geometry described in the above table. Table 4.6 lists the normalized stress results of each ply for the laminate under tension. As indicated, all of the models give no difference in stress results for a symmetric and balanced laminate without hole.

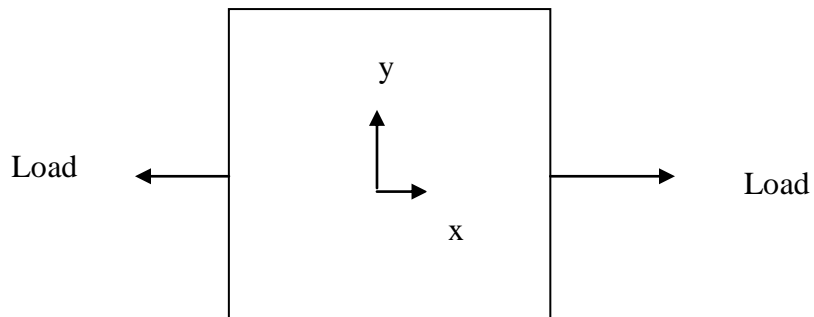


Figure 4.3 Plate in tension load

Table 4.6 Comparison between 2d Symmetric full model and quarter model

Symmetric layup (Stress normalized)									
	CLT			2 D Full model			2D quarter model		
	σ_x	σ_y	τ_{xy}	σ_x	σ_y	τ_{xy}	σ_x	σ_y	τ_{xy}
45	0.633	0.366	0.417	0.633	0.366	0.417	0.633	0.367	0.417
-45	0.633	0.366	-0.417	0.633	0.366	-0.417	0.633	0.367	-0.417
0	2.559	-0.009	0	2.559	-0.009	0	2.559	-0.009	0
90	0.174	-0.724	0	0.174	-0.724	0	0.174	-0.724	0
90	0.174	-0.724	0	0.174	-0.724	0	0.174	-0.724	0
0	2.559	-0.009	0	2.559	-0.009	0	2.559	-0.009	0
-45	0.633	0.366	-0.417	0.633	0.366	-0.417	0.633	0.367	-0.417
45	0.633	0.366	0.417	0.633	0.366	0.417	0.633	0.367	0.417

Table 4.7 Comparison between 2d Un- Symmetric full model and quarter model

Un-symmetric layup (Stress normalized)									
	CLT			2 D Full model			2D quarter model		
	σ_x	σ_y	τ_{xy}	σ_x	σ_y	τ_{xy}	σ_x	σ_y	τ_{xy}
45	0.478	0.073	0.205	0.478	0.073	0.205	0.472	0.067	0.197
-45	0.642	0.266	-0.396	0.642	0.266	-0.396	0.653	0.276	-0.407
0	2.925	-0.050	-0.005	2.925	-0.050	-0.005	2.931	-0.05	-0.007
90	0.186	-1.130	0.0	0.186	-1.131	0.0	0.186	-1.131	-0.001
45	0.664	0.373	0.442	0.664	0.373	0.442	0.651	0.360	0.427
-45	0.586	0.323	-0.362	0.586	0.323	-0.362	0.603	0.340	-0.381
0	2.445	0.009	0.016	2.445	0.009	0.016	2.449	0.009	0.013
90	0.166	-0.202	0.021	0.166	-0.202	0.021	0.167	-0.202	0.018

Table 4.7 lists the normalized stress of each ply for an un-symmetric layup analyzed by a full and a half finite element models of ANSYS. The results of laminate analysis by lamination theory are also included in the table for comparison. It is shown that only the stress results by 2D full model agree with the results obtained from classical lamination theory. However, the results obtained by a quarter-model show a slight difference from the results by classical lamination theory for an unsymmetrical laminate. It is well known that an unsymmetrical laminate subjected to a tension load gives an induced out-of-plane displacement. When a quarter-model is used, an out-of-plane displacement along the symmetrical edges of the model was suppressed. Hence, a quarter-model is not a truly representative of a unsymmetrical laminate under tension.

4.3 Full and Quarter of Three- Dimensional Models

It is known that a plane stress condition is enforced when a two-dimensional analysis is employed. That means, the stresses in z-direction are ignored. Since the state of the stress near free edge region is three-dimensional, a three-dimensional analysis is needed. Moreover, if the inter-laminar stresses are of interest for laminate under loading, a three-dimensional analysis is required. In conducting three-dimensional analysis, a plane strain condition is used. The following describes the stress effect of laminate with and without hole subjected to a tension load. Tables 4.8 and 4.9 summarize the normalized stress of each ply for laminate with a symmetric and unsymmetrical layup, respectively. A results obtained by a full 2D model is also included for comparison. The location of the ply stresses selected for the comparison is away from the edge to avoid the edge stress effect. Table 4.8 indicates that there is a negligible stress result difference between 2D model and 3D full model. This difference is contributed to the plane stress condition used in 2D model and the plane strain condition used in 3D model. There is also a negligible stress difference between 3D full model and quarter model. However, the stress difference between +45 and – 45 ply is observed. The results in Table 4.9 indicate

that a non-negligible difference of the ply stresses among all of the models. It is clearly shown that an induced bending for unsymmetrical laminate under tension is more produced in all of the models.

Table 4.8 Comparison between 3d Symmetric full model and quarter model (Plate without Hole)

Symmetric layup (Stress normalized)									
	2D Full model			3 D Full model			3D quarter model		
	σ_x	σ_y	τ_{xy}	σ_x	σ_y	τ_{xy}	σ_x	σ_y	τ_{xy}
45	0.633	0.366	0.417	0.634	0.362	0.418	0.625	0.357	0.412
-45	0.633	0.366	-0.417	0.634	0.368	-0.418	0.637	0.368	-0.420
0	2.559	-0.009	0	2.562	-0.011	0	2.579	-0.01	0
90	0.174	-0.724	0	0.174	-0.719	0	0.176	-0.739	0
90	0.174	-0.724	0	0.174	-0.719	0.001	0.176	-0.735	0
0	2.559	-0.009	0	2.562	-0.011	0	2.577	-0.010	0
-45	0.633	0.366	-0.417	0.634	0.368	-0.418	0.637	0.367	-0.419
45	0.633	0.366	0.417	0.634	0.362	0.418	0.622	0.358	0.406

Table 4.9 Comparison between 3D Un- Symmetric full model and quarter model (without hole)

Un-symmetric layup(Stress normalized)									
	2D Full model			3 D Full model			3D quarter model		
	σ_x	σ_y	τ_{xy}	σ_x	σ_y	τ_{xy}	σ_x	σ_y	τ_{xy}
45	0.478	0.073	0.205	0.481	0.071	0.206	0.520	0.132	0.248
-45	0.642	0.266	-0.396	0.637	0.257	-0.389	0.618	0.278	-0.374
0	2.925	-0.050	-0.005	2.935	-0.50	-0.004	2.810	-0.036	-0.002
90	0.186	-1.130	0	0.186	-1.145	0	0.181	-0.9	-0.001
45	0.664	0.373	0.442	0.660	0.369	0.438	0.698	0.367	0.485
-45	0.586	0.323	-0.362	0.587	0.325	-0.364	0.615	0.382	-0.405
0	2.445	0.009	0.016	2.434	0.010	0.015	2.283	0.026	0.011
90	0.166	-0.202	0.021	0.165	-0.189	0.020	0.156	-0.258	0.027

4.4 Full and Quarter Of Two- Dimensional Models of Laminate with a Hole

A laminated plate of 5 inch*2 inch has been used with a circular hole at the center of diameter 0.25 inch. First a 2 dimensional model will be discussed. The maximum ply stresses of a laminate with a hole obtained from a 2D model are shown in Figure 4.10.

Table 4.10 Comparison between 2d Symmetric full model and quarter model

Symmetric layup (Plate with a hole)						
	2 D Full model (Stress normalized)			2D quarter model (Stress normalized)		
θ	$ \sigma_x^{\max} $	$ \sigma_y^{\max} $	$ \tau_{xy}^{\max} $	$ \sigma_x^{\max} $	$ \sigma_y^{\max} $	$ \tau_{xy}^{\max} $
45	2.781	2.286	2.468	1.923	1.122	1.270
-45	2.781	2.286	2.468	2.781	2.286	2.468
0	7.731	0.082	0.229	7.731	0.082	0.229
90	0.528	2.607	0.229	0.528	2.607	0.229
90	0.528	2.607	0.229	0.528	2.607	0.229
0	7.731	0.082	0.229	7.731	0.082	0.229
-45	2.781	2.286	2.468	2.781	2.286	2.468
45	2.781	2.286	2.468	1.923	1.122	1.270

From the above table, it can be seen that the stress variation in the 2D quarter model and full model for +450 and - 450 plies for laminate with a hole. It is reminded that the peak stress always occurs at the location of the edge of the hole where the fiber is tangential to the hole. The quarter model of 2D shown in the above table is taken in the first quadrant of the laminate. The tangential location of +450 ply to the edge of the hole is out of the model domain. Hence, the peak stress of this ply is not a truly representative value. A comparison of the normalized peak stress results in global direction and fiber direction is also tabulated in Table 4.11. It can be seen from the table that for angle plies the fiber directional stress is higher. For zero degree layup the stress value does not change because for zero degree fiber direction is

actually in x direction. For a 2D model the location of peak stress for +45 and -45 degree are respectively at -45 degree and +45 degree from the x axis. For 00 ply it makes 900 and for 900 it makes 00 with x axis. It should also be noted that in table 4.11 the 900 y directional peak stress is actually showing compression.

Table 4.11 2D Symmetric full model normalized stress in x-y direction and fiber direction

Symmetric layup (Plate with a hole)						
	2 D Full model (x-y)			2 D Full model (1-2)		
θ	$ \sigma_x^{\max} $	$ \sigma_y^{\max} $	$ \tau_{xy}^{\max} $	$ \sigma_1^{\max} $	$ \sigma_2^{\max} $	$ \tau_{12}^{\max} $
45	2.781	2.286	2.468	4.983	0.358	0.400
-45	2.781	2.286	2.468	4.983	0.358	0.400
0	7.731	0.082	0.229	7.731	0.82	0.229
90	0.528	2.607	0.229	2.607	0.528	0.229
90	0.528	2.607	0.229	2.607	0.528	0.229
0	7.731	0.082	0.229	7.731	0.082	0.229
-45	2.781	2.286	2.468	4.983	0.358	0.400
45	2.781	2.286	2.468	4.983	0.358	0.400

Table 4.12 lists the normalized stress for laminate with an un-symmetric layup. The normalized stress values are shown in global x-y coordinate system for both full model and quarter model. The peak stress results of a full and a quarter 2D models are listed. As expected, significant difference of the results are observed between a full and a quarter model. This attributes the additional moment is enforced to a quarter model to suppress the induced

curvature due to unsymmetrical behavior.

Table 4.12 Comparison between 2d Un- Symmetric full model and quarter model

Un-Symmetric layup (Plate with a hole)						
	2 D Full model (Stress normalized)			2D quarter model (Stress normalized)		
	$ \sigma_x^{\max} $	$ \sigma_y^{\max} $	$ \tau_{xy}^{\max} $	$ \sigma_x^{\max} $	$ \sigma_y^{\max} $	$ \tau_{xy}^{\max} $
45	2.296	1.775	1.963	1.550	0.579	0.786
-45	2.628	2.127	2.304	2.608	2.097	2.272
0	7.982	0.229	0.226	8.570	0.249	0.221
90	0.542	3.131	0.246	0.544	3.367	0.235
45	3.161	2.621	2.844	2.085	1.320	1.471
-45	3.057	2.544	2.744	2.903	2.432	2.624
0	8.071	0.154	0.339	7.164	0.164	0.278
90	0.588	1.869	0.370	0.488	1.824	0.292

For a symmetric layup, (table 4.10) it was seen that the difference between 2D full model and quarter model was only at 45⁰ lamina. But for an un-symmetric layup (4.12) it can be seen that there is stress difference in all the lamina. Because of the un-symmetric layup there exists a coupling effect to extension loading. And this has been restrained by the quarter model boundary constraint. As a result quarter model is incapable of showing an actual result.

Table 4.13 shows the maximum stress result comparison between a full 2D and a quarter 2D for an un-symmetric layup in fiber direction.

Table 4.13 Comparison between 2d Un- Symmetric full model fiber direction results

Un-Symmetric layup (Plate with a hole)						
	2 D Full model (Stress normalized)			2D Full model (Stress normalized)		
	$ \sigma_x^{\max} $	$ \sigma_y^{\max} $	$ \tau_{xy}^{\max} $	$ \sigma_1^{\max} $	$ \sigma_2^{\max} $	$ \tau_{12}^{\max} $
45	2.296	1.775	1.963	3.986	0.325	0.495
-45	2.628	2.127	2.304	4.649	0.310	0.471
0	7.982	0.229	0.226	7.982	0.210	0.226
90	0.542	3.131	0.246	2.816	0.542	0.246
45	3.161	2.621	2.844	5.733	0.376	0.402
-45	3.057	2.544	2.744	5.542	0.445	0.379
0	8.071	0.154	0.339	8.072	0.134	0.339
90	0.588	1.869	0.370	1.578	0.588	0.370

Result summary: From the above tables (4.10-4.13), it is seen that for the symmetric layup no bending is induced as the layer stresses in the top layers from mid-plane are the mirror image of the bottom layers. However, bending is induced in the un-symmetric layup.

The hole at the middle of the plate will take an elliptical shape due to tension loading. The following figure will show the deformation of the hole due to tension loading. The x and y coordinate values have been obtained from the FEM geometry.

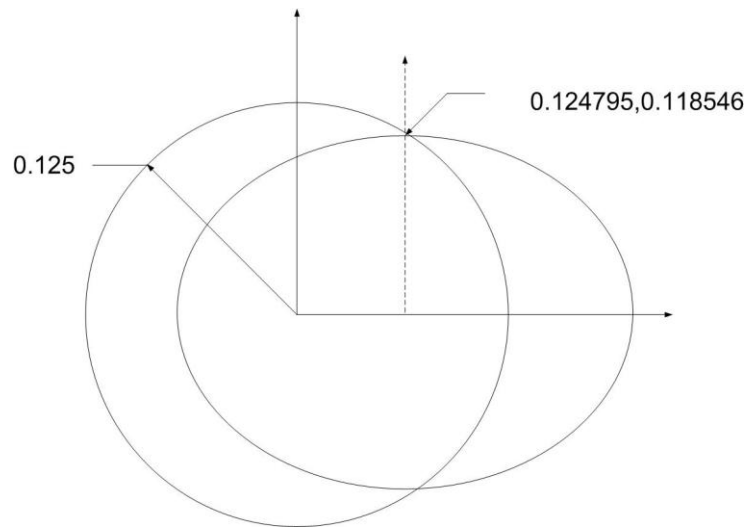


Figure 4.4 Deformation of 2d plate with a hole full model

From the above figure, the new origin is at (0.124795,0) after deformation. The following table will show the location of maximum stresses for the layers of symmetric laminate from the table 4.10.

Table 4.14 Location of maximum stress for 2d symmetric full model

layup	$\theta = \tan^{-1} \frac{y}{x}$
45	-68.58
-45	68.58
0	90
90	90

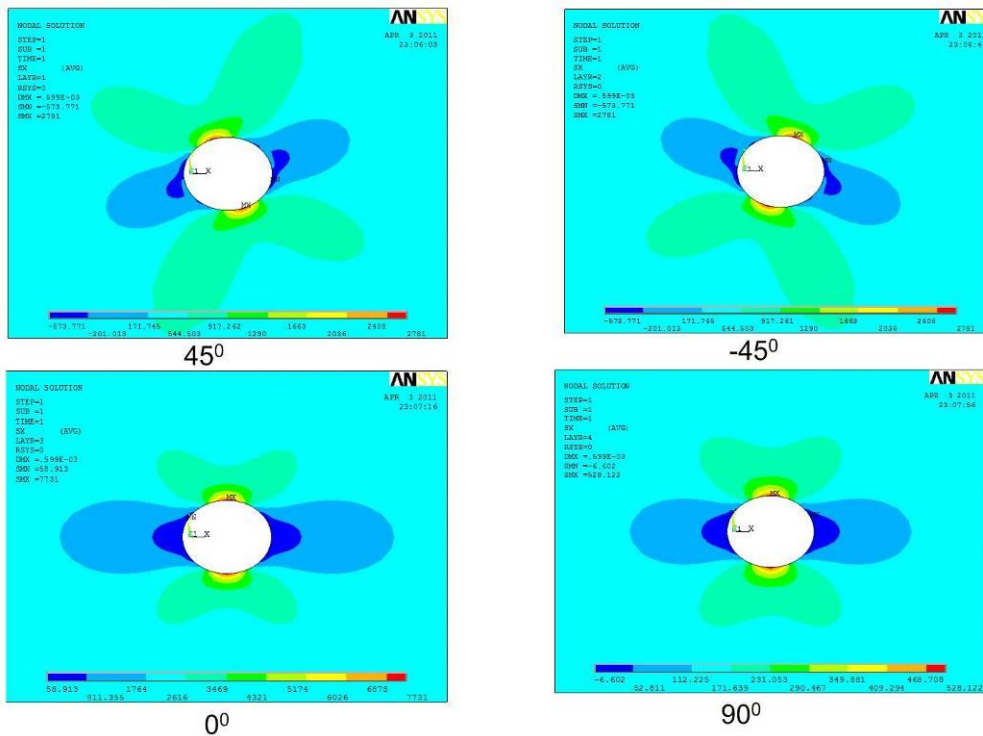


Figure 4.5 maximum stress of 2d plate with a hole full model

From the above figure and table it can be clearly concluded that the maximum stress always happen to tangential to the fiber direction. Now for a quarter model the origin is not displaced from its location because a symmetric constraint is applied. The deformation of the model is shown in the following figure. The value of the coordinate point after deformation has been obtained from the FEM model.

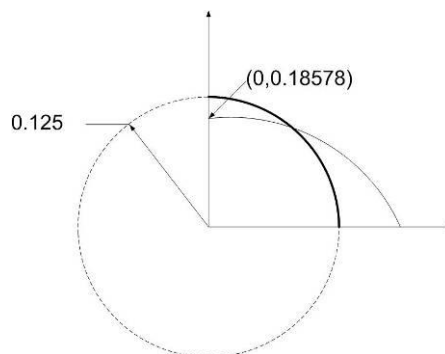


Figure 4.6 Deformation of 2d plate with a hole quarter model

For a quarter model in the first quadrant, it is seen that the positive 45 degree x directional maximum stress does not assume the same value as a full model. More over the position of the maximum stress is at 90 degree. Whereas for a full model the x directional maximum stress for a positive 45 degree layer is at negative 68.58 degree. On the other hand the maximum x directional stress value and location remain same for the negative 45 degree lamina for both quarter and full model. To describe this phenomenon the resultant location has been tabulated first. The following table will show the resultant location of the maximum stress angle for a quarter model in the first quadrant.

Table 4.15 Location of maximum stress for 2d symmetric quarter model

Layup	$\theta = \tan^{-1} \frac{y}{x}$
45	90
-45	68.50
0	90
90	90

From the above figure and table it is clearly seen that for positive 45⁰ lamina the location of the maximum stress in x direction (loading direction) is at 90⁰ and from table 4.10 it is seen that the maximum stress value for x direction differs from the full model value. From the full model it has been also confirmed that maximum stress always occurs tangential to the fiber direction but the tangential location for a positive 45⁰ layer is not present in the quarter model because of the symmetric constrained applied in the quarter model. That is why the maximum stress is assuming a nearest point which is 90⁰ and the value of the x directional maximum stress is much lower than the full model value. Figure 4.8 describe the effect more elaborately.

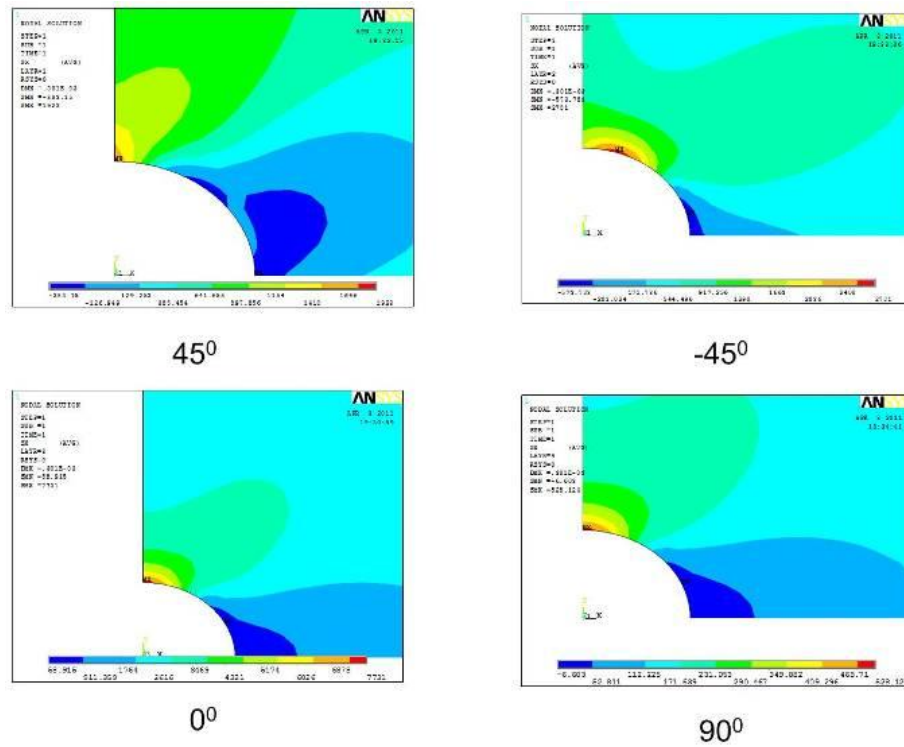


Figure 4.7 Maximum stress of 2d plate with a hole quarter model

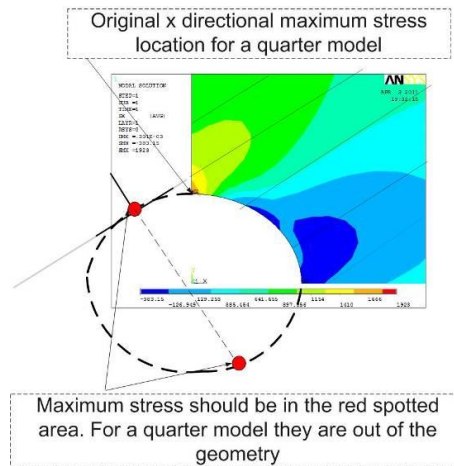


Figure 4.8 Maximum stress of 45 degree lamina in with a hole 2D quarter model

The similar effect is for y directional maximum stress of + 45⁰ lamina. The other laminas with 0⁰, 90⁰, - 45⁰ fiber direction shows same result as in full model. In the boundary condition

chapter it will be shown that for a quarter models in different quadrant the + 45° and negative 45° stress result is swapped.

For as un-symmetric layup the full model and quarter model result for maximum stress is quite different. This effect has been discussed in the earlier section with a 2d plate without a hole model. In brief as symmetric constrained is applied in quarter model, it is actually restraining the curvature. As a result the result for 2d quarter model and full model varies much.

The following table will show the result of a plate with a hole model in 3 D space. A plate of 5 inch*2 inch has been used with a circular hole at the center of diameter 0.25 inch. Each layer has a ply thickness of 0.005 inch.

Table 4.16 Comparison between 3d Symmetric (with hole) full model and quarter model

θ	3 D Full model (stress normalized)			3D quarter model (stress normalized)		
	$ \sigma_x^{\max} $	$ \sigma_y^{\max} $	$ \tau_{xy}^{\max} $	$ \sigma_x^{\max} $	$ \sigma_y^{\max} $	$ \tau_{xy}^{\max} $
45	2.320	1.707	1.929	1.868	1.245	1.236
-45	2.484	1.909	1.000	2.436	1.873	2.333
0	9.965	0.403	0.790	10.259	0.294	0.827
90	0.837	3.217	0.698	0.901	3.130	0.689
90	0.837	3.217	0.698	0.901	3.130	0.689
0	9.965	0.403	0.790	10.259	0.294	0.827
-45	2.484	1.909	1.000	2.436	1.873	2.333
45	2.320	1.707	1.929	1.868	1.245	1.236

From table 4.16 it can be seen that there is a noticeable difference in 45° lamina. Because the peak stress location for 45° laminate is out of the quarter model geometry. There is also a difference in the stress result of other lamina because of the edge stress effect. As there is a discontinuity in the geometry and peak stress is considered the difference is more than that of an un-notched result.

The next table will show the fiber directional peak stress result for a plate with a hole symmetric layup.

Table 4.17 3d Symmetric full model stress in fiber direction

Symmetric layup (Plate with a hole)						
θ	3 D Full model (stress normalized)			3 D Full model (stress normalized)		
	$ \sigma_x^{\max} $	$ \sigma_y^{\max} $	$ \tau_{xy}^{\max} $	$ \sigma_1^{\max} $	$ \sigma_2^{\max} $	$ \tau_{12}^{\max} $
45	2.320	1.707	1.929	3.921	0.543	0.670
-45	2.484	1.909	1.000	4.538	0.879	0.617
0	9.965	0.403	0.790	9.965	0.403	0.790
90	0.837	3.217	0.698	3.217	0.837	0.698
90	0.837	3.217	0.698	3.217	0.837	0.698
0	9.965	0.403	0.790	9.965	0.403	0.790
-45	2.484	1.909	1.000	4.538	0.879	0.617
45	2.320	1.707	1.929	3.921	0.543	0.670

For a 2D model (Table 4.11) it was shown that the fiber directional result for $\pm 45^\circ$ was same for a symmetric layup. But for 3D model there is a variation because an inter-laminar stress is acting at the edge. The location of the peak stress is shown in the following table.

Table 4.18 Peak stress location of 3D symmetric full model in fiber direction

layup	$\theta = \tan^{-1} \frac{y}{x}$
45	-48
-45	46
0	90
90	0

It can be seen from the table that for $[\pm 45]$ lamina the peak stress occurs at a tangential location. For 0° lamina it occurs at 90° which is the tangential location for 0° . For 90° lamina the peak stress is actually a compression and it also occurs at a tangential location. The following table will show the 3D full model and quarter model result for an un-symmetric layup. Same like symmetric layup there is a large variation of stress result for 45° lamina. As has been discussed before there is a bending induced (it can be seen that for un-symmetric layup the top 0° lamina has a higher stress value than the bottom 0° lamina. This proves that there is a bending present) for un-symmetric layup which has been restrained by the symmetric constraint in a quarter model. So there exists a variation of result in the other laminas. For an un-symmetric layup for 3d model the bending effect is less than the bending effect for a 2D model. Because a 2D model is softer than a 3D model (2D model uses a reduced stiffness matrix). But the 2D model does not count for the edge effect and inter-laminar stress.

Table 4.19 Comparison between 3d Un- Symmetric full model and quarter model (with hole)

	3 D Full model (Stress normalized)			3D quarter model (Stress normalized)		
	$ \sigma_x^{\max} $	$ \sigma_y^{\max} $	$ \tau_{xy}^{\max} $	$ \sigma_x^{\max} $	$ \sigma_y^{\max} $	$ \tau_{xy}^{\max} $
45	2.117	1.459	1.676	1.967	1.176	1.245
-45	2.520	1.912	2.410	2.568	1.951	2.444
0	10.128	0.396	0.812	10.849	0.328	0.827
90	0.899	3.906	0.690	0.981	3.940	0.676
45	2.581	2.059	2.155	1.686	1.121	1.107
-45	2.452	1.888	2.359	2.289	1.763	2.209
0	9.652	0.414	0.810	8.927	0.267	0.734
90	0.740	2.079	0.675	.742	2.790	0.611

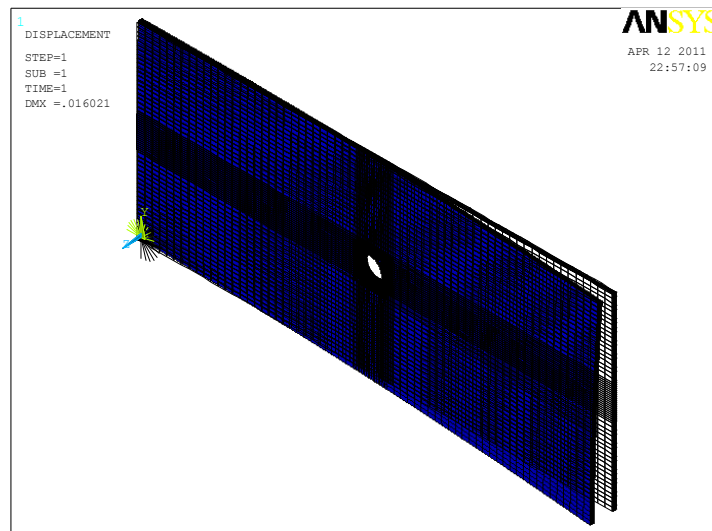


Figure 4.9 Deformed shape of a 3d plate with hole

Table 4.20 Comparison between 3d Un- Symmetric full model in fiber direction

Un-Symmetric layup (Plate with a hole)						
	3 D Full model (Stress normalized)			3D full model (Stress normalized)		
	$ \sigma_x^{\max} $	$ \sigma_y^{\max} $	$ \tau_{xy}^{\max} $	$ \sigma_1^{\max} $	$ \sigma_{1-1}^{\max} $	$ \tau_{1-2}^{\max} $
45	2.117	1.459	1.676	3.405	0.573	0.623
-45	2.520	1.912	2.410	4.554	0.886	0.639
0	10.128	0.396	0.812	10.128	0.395	0.812
90	0.899	3.906	0.690	3.906	0.899	0.690
45	2.581	2.059	2.155	4.402	0.479	0.634
-45	2.452	1.888	2.359	4.497	0.854	0.601
0	9.652	0.414	0.810	9.652	0.414	0.810
90	0.740	2.079	0.675	0.2079	0.739	0.675

Table 4.21 Peak stress location of 3D un-symmetric full model in fiber direction

layup	$\theta = \tan^{-1} \frac{y}{x}$
45	-53
-45	57
0	90
90	0

From the table 4.16 it was seen that for a symmetric full model the stresses above the mid plane is a mirror image of stresses below the mid plane. As a result no bending is induced for a symmetric lamina when axial load is applied. On the other hand bending is induced in an un-symmetric layup. For a quarter symmetric model (table 4.16), the result varies from symmetric full model for a 45 degree lamina. The reason is already been described in 2d model result. In brief the reason behind this variation in 45 degree lamina is a symmetric constraint has been applied in the quarter model. As 45 degree lamina stress is different in symmetric full model and quarter model, unlike 2d model it affects the stress result in other lamina too because of the inter laminar stress is considered in a 3d model. This stress effect is not big for a thin lamina as a result the effect of stress variation of 45 degree lamina on other lamina is very small. In case of thick lamina the effect will be more pronounced. The resultant location of the maximum stress in x direction for different lamina is shown in the following figure.

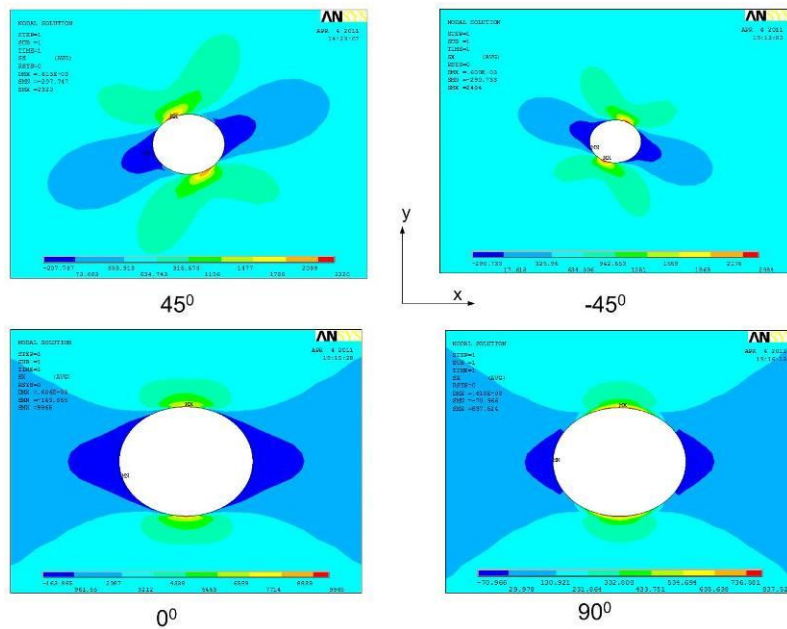


Figure 4.10 Maximum stress of 3d plate with a hole full model (x directional load)

From the above figure it is clearly seen that the maximum stress always occurs tangential to the fiber direction. The following table will show the value of maximum stress location angle with

respect to x axis.

Table 4.22 Location of maximum stress for 3d symmetric full model and quarter model

Layup	$\theta = \tan^{-1} \frac{y}{x}$	$\theta = \tan^{-1} \frac{y}{x}$
45	-53.24	90
-45	58.47	58.26
0	90	90
90	90	90

The following figure will show the x directional maximum stress location for different lamina of a 3D symmetric quarter model. It is seen from the figure that the + 45° layer x directional peak stress is in a 90° angle with x axis. The tangential location of a + 45 degree lamina where the peak stress supposed to occur, is out of the geometry of a first quadrant As a result the maximum stress assumes a location 90° with respect to x axis.

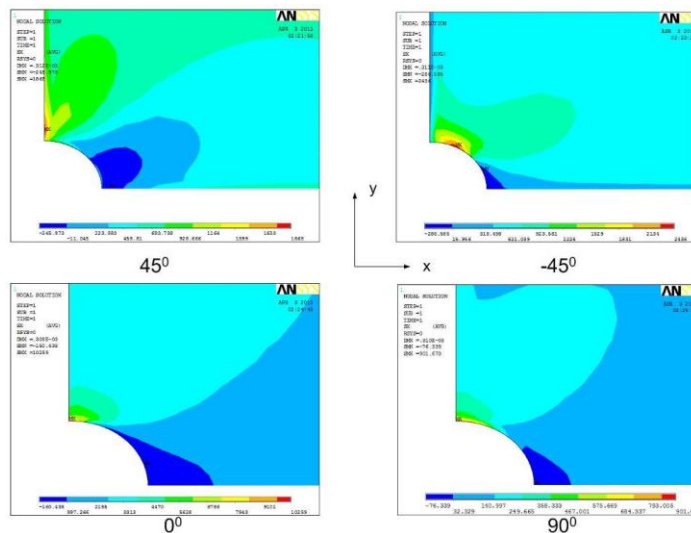


Figure 4.11 Maximum stress of 3d plate with a hole quarter model (x directional load)

4.5 Lumping layer Theory

Because of the aspect ratio issue discussed in the mesh chapter it requires a large number of elements for a composite three dimensional model. Such a large number of element will result in cost, computational time. So there should be some way to minimize cost and time. As a result lumping layer theory was developed. Chan and his students [4] have done numerous amount of work in this field. As a discussion of finite element issues, lumping layer theory should also need to be summarized in this dissertation. In order to discuss the lumping layer effect a $[\pm 45/0/90]_s$ layup has been used, The equivalent property table is shown below,

Table 4.23 Equivalent Property Table for Lumped Layers

$[\pm 45/0/90]_s$	10^6	E_x Msi	E_y Msi	ν_{xy}	G_{xy} Msi
$[\pm 45]$ lumped, $[\bar{0}/0/90]_s$	Conventional	2.6252	2.6252	0.5084	2.4934
	Modified	3.0439	3.0439	0.7490	5.6628
$[\pm 45/0]$ lumped. $[\bar{0}^-/0/90]_s$	Conventional	4.6428	2.5886	0.6118	2.4396
	Modified	9.3985	4.0706	0.6973	4.0653

Both the conventional method and modified method [4] has been used to calculate the equivalent properties of the lumped layers. I can be seen from the above table that the conventional equivalent properties are different from the modified method. The variation is more significant for an unbalanced laminate. In this thesis only $[\pm 45]$ laminate results for stress has been considered. The stress value for the lumped $[\pm 45]$ layers and the other layers has been tabulated in the following table. The result is compared to the classical lamination theory analysis of the full model. It is seen from the table that for a not lumped layer the present modified method gives better result.

Table 4.24 Lumping Layer Technique Table

	Lumped(present method)			Not lumped			Lumped(conventional method)		
	σ_x	σ_y	τ_{xy}	σ_x	σ_y	τ_{xy}	σ_x	σ_y	τ_{xy}
45	Lumped	Lumped	Lumped,0	634	362	418	Lumped	Lumped	Lumped
-45	Lumped	Lumped	Lumped,0	634	368	-418	Lumped,	Lumped	Lumped
0	2560	-9	0	2562	-11	0	2909	22	0
90	175	-716	0	174	-719	0.8	206	-366	0
90	175	-716	0	174	-719	1.3	206	-366	0
0	2560	-9	0	2562	-11	0	2909	22	0
-45	Lumped	Lumped	Lumped,0	634	368	-418	Lumped,	lumped	lumped
45	Lumped,	Lumped	Lumped,	634	362	418	Lumped	lumped	lumped

In the following table the stress of the lumped layer has been recovered by using the conventional method and Modified method. The layer stress recovery technique has been modified by Chan and his students [8]. It can be clearly seen from the table that the modified method gives better result in comparison to the conventional method. This is because, in conventional method the curvature effect and the shear correction was not included. But for an un-symmetric and unbalanced lamina these effects plays a vital role. In the table below the [± 45] layers have been lumped together. This is an Un-symmetric layup. So shear is induced. This effect has been taken care of in the modified method.

Table 4.25 Lumping Layer Recovery Technique Table

	Stress Recovery Lumped(present method)			Not lumped			Stress Recovery Lumped(conventional method)		
	σ_x	σ_y	τ_{xy}	σ_x	σ_y	τ_{xy}	σ_x	σ_y	τ_{xy}
45	634	359	418	634	362	418	824	559	577
-45	634	359	-418	634	368	-418	824	559	-577
0	2560	-9	0	2562	-11	0	2909	22	0
90	175	-716	0	174	-719	0.8	206	-366	0
90	175	-716	0	174	-719	1.3	206	-366	0
0	2560	-9	0	2562	-11	0	2909	22	0
-45	634	359	-418	634	368	-418	824	559	-577
45	634	359	418	634	362	418	824	559	577

CHAPTER 5

BOUNDARY CONDITIONS

In this chapter effect of boundary constraints on the ply stresses will be discussed. In modeling, symmetric conditions of structures made of isotropic materials are usually enforced. However, symmetric conditions of structures made of anisotropic materials must be considered the symmetry of materials axis.

5.1 Structural Response of 2D model

A 2D quarter-model of a laminate with different kind of layups (symmetric/un-symmetric and balanced/unbalanced) is used to study the symmetric constraint effects on the result of finite element analyses of composite materials. A composite laminate under tension load is used in this study. This method was done on balanced/unbalanced laminate by Chen [5]. It's been extended to symmetric/unsymmetrical laminate. The displacement of the laminate were obtained by the elasticity method and given as,

$$\begin{aligned} u(x, y) &= \left(a_{11}x + \frac{a_{16}}{2} y \right) N_x \\ v(x, y) &= \left(\frac{a_{16}}{2} x + a_{12}y \right) N_x \end{aligned} \tag{5.1}$$

As indicated in Table 5.1, the FEM results of symmetric and balanced laminate agree well with the elastic solution. It is aware that a smeared property from ANSYS was used in stress calculations. Hence, for a symmetrical laminate, the material axis is symmetric. As a result, the quarter model will give the same results as a full model which is expected to be the same from the results calculated by closed form solution. However, there is a big difference for the symmetric but unbalanced laminates. There is also difference in unsymmetrical but

balanced laminate. This is because additional forces and moments were induced when symmetrical constraints were enforced.

Table 5.1 Comparison of Normalized Displacement

Lay ups		10-6	Point A (x=0.25 y=0.25)		Point B (x=0 y=0.25)		Point C (x=0.25 y=0)	
			Eqn	Fem	Eqn	Fem	Eqn	Fem
symmetric	[±45/0/90]s	u	29.411	29.4	0	0	29.4	29.4
		v	8.83	8.83	8.83	8.83	0	0
Un-symmetric	[±45/0/90]t	u	31.71	31.3	0.8	0	30.9	30.4
		v	10.06	10.5	10.85	11.3	0.8	0
Balanced	[±45]2s	u	82.1	82.1	0	0	82.1	82.1
		v	61.5	61.5	61.5	61.5	0	0
unbalanced	[45 ₂]2s	u	76.1	85.8	36.3	0	112.4	129
		v	67.5	57.8	31.2	15.0	36.3	0

5.2 Maximum stress of laminate with hole by full 3D and a quarter 3D

Stress effects due to boundary constraints in a 3d model also depend on laminate configuration and the principle material axis. A symmetrical graphite/epoxy laminate of [±45/0/90]s with a rectangular cross section and a hole at the center under tensile load was used to study this effect using quarter and full models. Table 5.2 lists the result comparison for layer stresses obtained by a quarter and full 3D model. Since no bending is induced for the symmetrical laminate under tension, only half of laminate stresses are presented. The table indicates that the corresponding stress components, σ_x and σ_y of 45° and -45° , respectively are not the same. As indicated in the table the results in the quarter 3D model has bigger difference than from the full 3D model.

Table 5.2 Stress distribution to show symmetric constraint effect

	Full 3D(solid)			Quarter 3D (solid)		
	σ_x	σ_y	τ_{xy}	σ_x	σ_y	τ_{xy}
45	2320	1707	1929	1868	1245	1236
-45	2484	1909	1000	2436	1873	2333
0	9965	403	790	10259	294	827
90	837	3217	698	901	3130	689

For the laminate with a circular cut out the stress effect is more pronounced for angle plies than an un-notched model. Figure 5.1 will show the difference of the maximum stress at 450 and -450 plies of $[\pm 45/0/90]_s$ laminate under tension obtained from a quarter and full model, respectively. It also indicates that the maximum stress occur at different locations. It is well known that for an isotropic plate with a hole the maximum stress at the edge of the hole obtained by FEM is not different between a quarter and a full model.

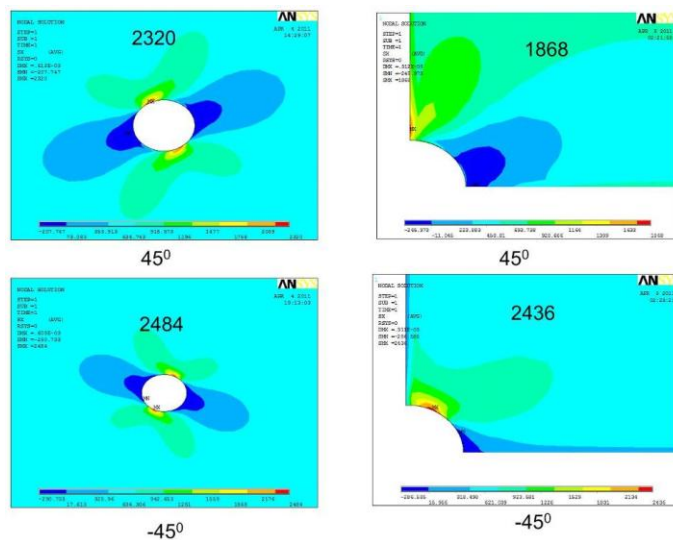


Figure 5.1 Stress Concentration Comparisons Of Quarter and Full 3D Model.

It is clear from the above figure that there is a considerable amount of difference in stress in angle ply in a three dimensional quarter model. The results in the figure were shown for a quarter models in the first quadrant.

5.3 Effect of boundary constraints locations

Figures 5.2 and 5.3 show the stress contours of the $+45^\circ$ and -45° ply in the same laminate in the different quadrants of 2D model, respectively. As indicated, the stress contour of the $+45^\circ$ ply shown in Fig. 5.2 is in the anti-symmetrical position in the quadrant positions. The stress contours in -45° ply at 2nd quadrant is the same as the stress contour of $+45^\circ$ ply in the first quadrant.

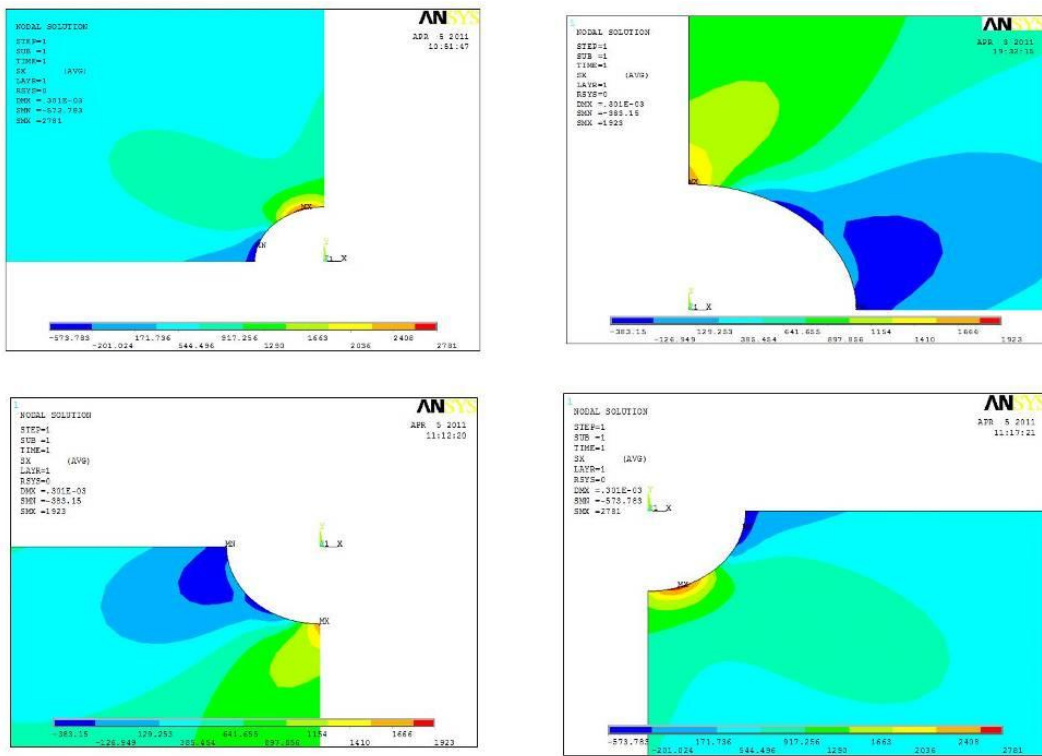


Figure 5.2 2D quarter model maximum stress in x direction for positive 45 degree layer

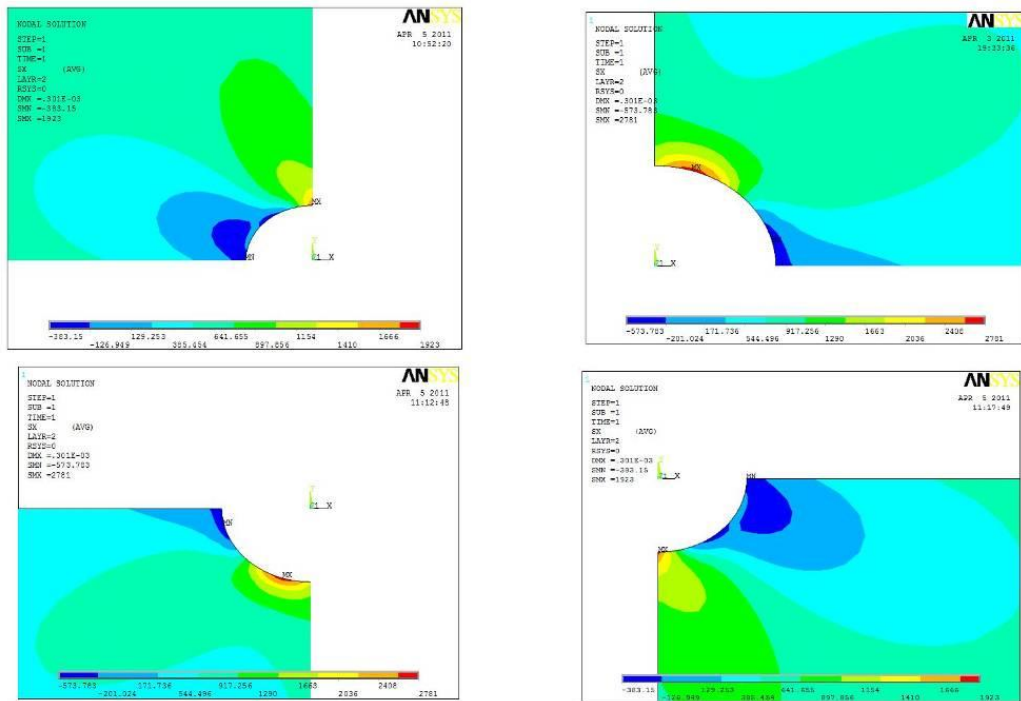


Figure 5.3 2D quarter model maximum stress in x direction for negative 45 degree layer

The numerical values of the normalized maximum stresses are listed in Table 5.3.

From the above table it can be seen that for the quarter-model in all four quadrant, the 00 and the 90° results are same for a symmetric layup of two dimensional quarter model. The figure shows that the maximum stress value for these layers occurs at 90° which is at tangential to the fiber direction.

Table 5.3 2D quarter swap effect (Stress normalized)

2 D Symmetric layup (Plate with a hole)															
	2 D Full model			first quad			second quadrant			3rd quadrant			4th quadrant		
θ	$ \sigma_x^{\max} $	$ \sigma_y^{\max} $	$ \tau_{xy}^{\max} $	$ \sigma_x^{\max} $	$ \sigma_y^{\max} $	$ \tau_{xy}^{\max} $	$ \sigma_x^{\max} $	$ \sigma_y^{\max} $	$ \tau_{xy}^{\max} $	$ \sigma_x^{\max} $	$ \sigma_y^{\max} $	$ \tau_{xy}^{\max} $	$ \sigma_x^{\max} $	$ \sigma_y^{\max} $	$ \tau_{xy}^{\max} $
45	2.781	2.286	2.468	1.923	1.122	1.270	2.781	2.286	2.468	1.923	1.122	1.270	2.781	2.286	2.468
-45	2.781	2.286	2.468	2.781	2.286	2.468	1.923	1.122	1.270	2.781	2.286	2.468	1.923	1.122	1.270
0	7.731	0.082	0.229	7.731	0.082	0.229	7.731	0.082	0.229	7.731	0.082	0.229	7.731	0.082	0.229
90	0.528	0.742	0.229	0.528	0.742	0.229	0.528	0.742	0.229	0.528	0.742	0.229	0.528	0.742	0.229
90	0.528	0.742	0.229	0.528	0.742	0.229	0.528	0.742	0.229	0.528	0.742	0.229	0.528	0.742	0.229
0	7.731	0.082	0.229	7.731	0.082	0.229	7.731	0.082	0.229	7.731	0.082	0.229	7.731	0.082	0.229
-45	2.781	2.286	2.468	2.781	2.286	2.468	1.923	1.122	1.270	2.781	2.286	2.468	1.923	1.122	1.270
45	2.781	2.286	2.468	1.923	1.122	1.270	2.781	2.286	2.468	1.923	1.122	1.270	2.781	2.286	2.468

But for the angle plies the results are varying. To be specific for the angle plies the results are exactly same only in the respectively diagonal quadrants. This is because by applying symmetric constraint in a sense the fiber orientation is also being changed. The following figure will describe the effect. It will be shown from the figure that positive 45 degree fiber orientation becomes a negative 45 degree orientation in a quarter model if the model is done in the second or fourth quadrant. This is the reason behind the swapping effect of stress in the angle ply in a quarter model.

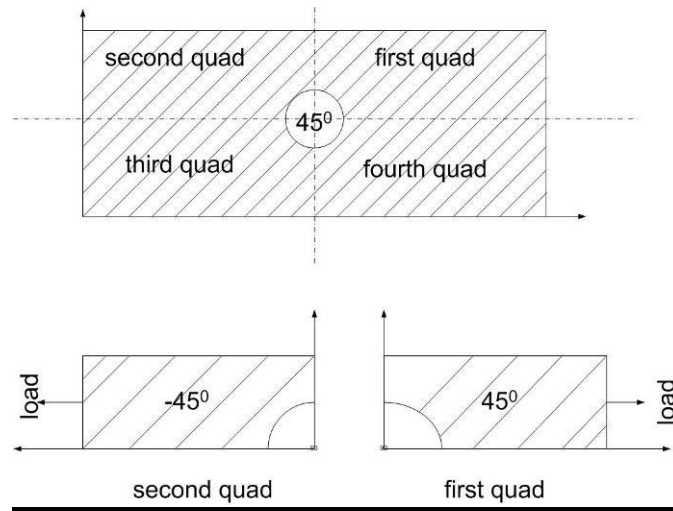


Figure 5.4 45 degree layup in full model becomes - 45 degree in 2nd quadrant quarter model

The same effects also appears in 3D quarter models. The results are presented in Figures 5.5 and 5.6 as well as in Table 5.4.

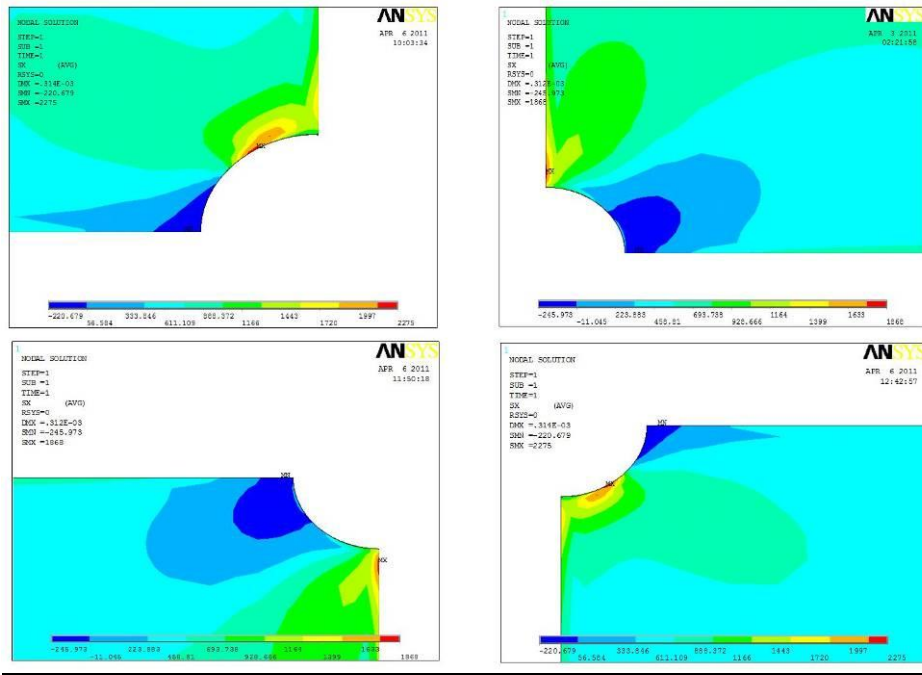


Figure 5.5 3D quarter model maximum stress in x direction for positive 45 degree layer

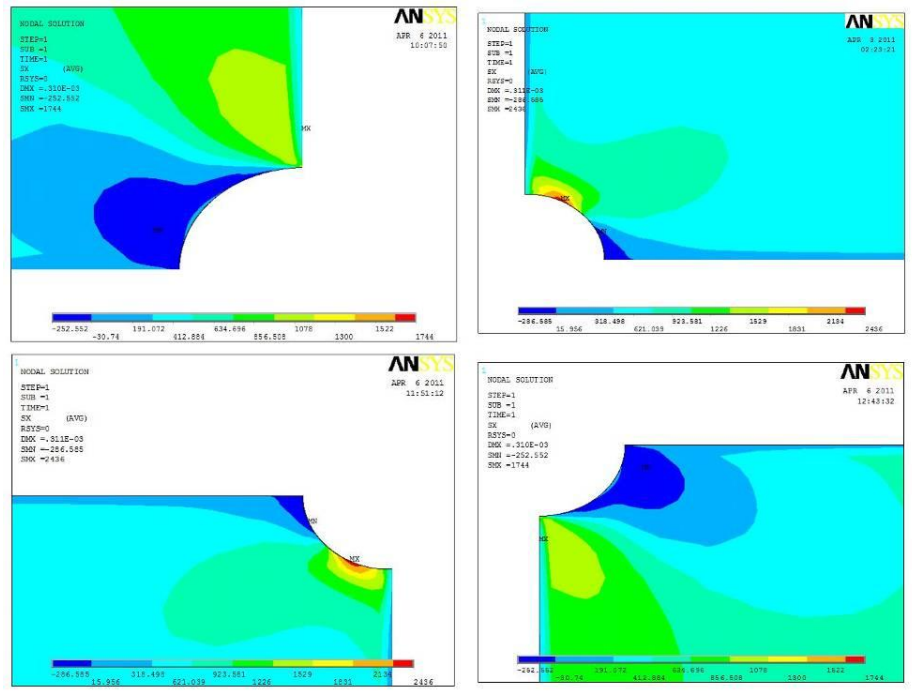


Figure 5.6 3D quarter model maximum stress in x direction for negative 45 degree layer

Table 5.4 3D quarter swap effect

3D Symmetric layup (Plate with a hole)															
	3 D Full model			first quad			second quadrant			3rd quadrant			4th quadrant		
θ	σ_x^{\max}	σ_y^{\max}	τ_{xy}^{\max}	σ_x^{\max}	σ_y^{\max}	τ_{xy}^{\max}	σ_x^{\max}	σ_y^{\max}	τ_{xy}^{\max}	σ_x^{\max}	σ_y^{\max}	τ_{xy}^{\max}	σ_x^{\max}	σ_y^{\max}	τ_{xy}^{\max}
45	2.320	1.707	1.929	1.868	1.245	1.236	2.275	1.674	1.892	1.868	1.245	1.236	2.275	1.674	1.892
-45	2.484	1.909	1.000	2.436	1.873	2.333	1.744	1.191	1.158	2.436	1.873	2.333	1.744	1.191	1.158
0	9.965	0.403	0.790	10.259	0.294	0.827	10.968	0.403	0.808	10.259	0.294	0.827	10.968	0.403	0.808
90	0.837	3.217	0.698	0.901	3.130	0.689	0.796	3.338	0.676	0.901	3.130	0.689	0.796	3.338	0.676
90	0.837	3.217	0.698	0.901	3.130	0.689	0.796	3.338	0.676	0.901	3.130	0.689	0.796	3.338	0.676
0	9.965	0.403	0.790	10.259	0.294	0.827	10.968	0.403	0.808	10.259	0.294	0.827	10.968	0.403	0.808
-45	2.484	1.909	1.000	2.436	1.873	2.333	1.744	1.191	1.158	2.436	1.873	2.333	1.744	1.191	1.158
45	2.320	1.707	1.929	1.868	1.245	1.236	2.275	1.674	1.892	1.868	1.245	1.236	2.275	1.674	1.892

5.4 Curved beam with symmetric layup [+45/0/90]s

This section discusses the stress effect due to the curvature of the laminate. A curved beam of [+45/-45/0/90]s laminate subjected to tension is used for this study. Figure 5.7 shows a deformed shape for a 3D model of the curved beam. As expected, an induced bending is observed when applied a tension.

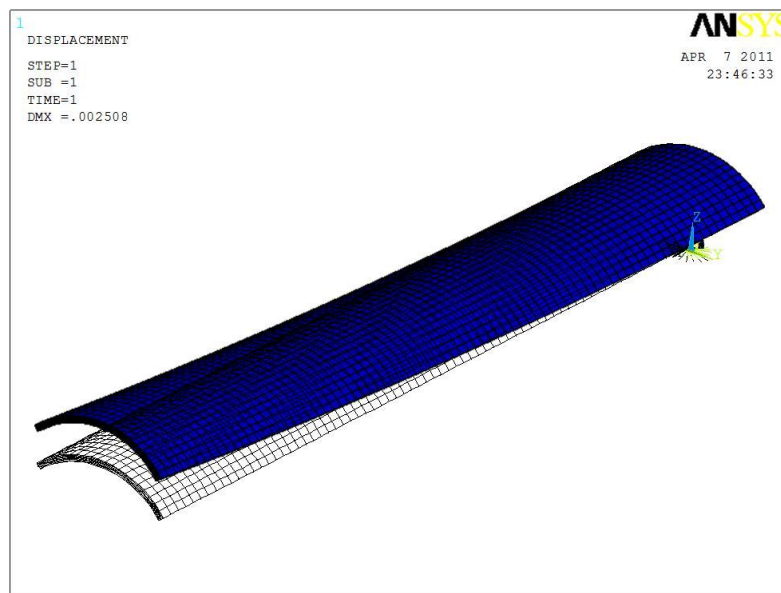


Figure 5.7 3D Curved Beam

Table 5.5 lists the stress results of the curved beam with difference curvatures. When curvature is increased the curved beam will start behaving like a flat plate. It can be seen from the table that for an increased curvature the zero degree x directional stress is decreased. It is observed that the bending effect induced by the curvature will start to diminish with increasing curvature.

Table 5.6 shows the aspect ratio effect for a curved beam. The aspect ratio has already been discussed in chapter 3. It's been shown that for composite three dimensional models, aspect ratio plays a vital role. For a curved beam the aspect ratio effect is more than in the flat

plate model. The table shows that the lower the aspect ratio, the better is the result.

Table 5.5 Curvature effect for 3d curved beam FEM model

R= 0.15	σ_x	σ_y	τ_{xy}
45	710	398	463
-45	713	379	-476
0	2897	-40	8
90	193	-955	6
90	192	-506	5.3
0	2870	11	4.6
-45	703	413	-469
45	686	358	463
R= 0.5	σ_x	σ_y	τ_{xy}
45	656	382	379
-45	604	402	-385
0	2704	-20	1.42
90	181.517	-693	1.07
90	179	-698	1.38
0	2620	-7	0
-45	667	402	-449
45	656	382	443
R= 5	σ_x	σ_y	τ_{xy}
45	642	373	420
-45	638	369	-419
0	2612	-11	0
90	177	-735	0
90	176	-717	0
0	2591	-9.2	0
-45	651	376	-429
45	644	370	422

Table 5.6 curved beam aspect ratio comparison

R=0.58	Model 1			Model 2			Model 3		
	No of element 12800			No of element 19200			No of element 43200		
	$\frac{\ell}{t_{ply}} = \frac{0.075}{0.005} = 15$			$\frac{\ell}{t_{ply}} = \frac{0.05}{0.005} = 10$			$\frac{\ell}{t_{ply}} = \frac{0.0333}{0.005} = 6.66$		
	σ_x	σ_y	τ_{xy}	σ_x	σ_y	τ_{xy}	σ_x	σ_y	τ_{xy}
45	618	328	395	641	354	416	669	386	448
-45	627	343	-400	647	365	-419	677	403	-453
0	2689	-7	1	2708	-7	0	2705	-2	0
90	183	-619	1	185	-673	0	185	-715	0
90	186	-882	1	186	-762	0	186	-872	0
0	2732	-16	1	2750	-15	0	2746	-18	0
-45	645	348	-411	660	362	-425	689	396	-458
45	648	355	412	663	369	427	694	408	460

A comparison of 2D and 3D models of a curved beam is illustrated in Table 5.7. It is shown that the 2D curved beam result agrees more to classical lamination theory analysis than a three dimensional model. Both CLT and two dimensional FEM models assume the plane stress condition. But the expression of constitutive equation for the curved beam does not take into account the effect of Poisson's ratio. So there exists some variations in two dimensional and lamination theory for a curved beam analysis. This variation between CTL and two dimensional FEM model was not seen in the case of a flat plate analysis because for a flat plate lamination theory analysis Poisson's ratio was included.

Table 5.7 2D and 3D curved beam comparison

R=0.58	CLT			3D model			2d Model		
	σ_x	σ_y	τ_{xy}	σ_x	σ_y	τ_{xy}	σ_x	σ_y	τ_{xy}
45	616	357	406	641	354	416	626	362	412
-45	622	360	-410	647	365	-419	630	366	-416
0	2537	-9	0	2709	-7	0	2538	-9	0
90	174	-724	0	185	-673	0	174	-718	0
90	176	-730	0	186	-762	0	174	-719	0
0	2603	-9	0	2750	-15	0	2543	-10	0
-45	644	373	-424	660	362	-425	627	361	412
45	650	376	428	663	369	427	631	366	-416

Table 5.8 lists the stress results of the curved beam using a 3 dimensional full model and a quarter model. It can be seen that the half model results varies much from the full model. This is because a symmetric constraint is applied for the half model. The reason has been already discussed in the boundary condition chapter.

Table 5.8 3D curved beam full versus quarter model comparison

R=0.58	3D full model			3D half model		
	σ_x	σ_y	τ_{xy}	σ_x	σ_y	τ_{xy}
45	641	354	416	626	311	410
-45	647	365	-419	680	358	-457
0	2709	-7	0	2725	-1	10
90	185	-673	0	196	-636	11
90	186	-762	0	186	-733	5
0	2750	-15	0	2758	-25	-6
-45	660	362	-425	645	339	-416
45	663	369	427	620	352	420

CHAPTER 6

CONCLUSION

This thesis addresses the issues that need special attention when using the finite element method in analyzing composite structures. Applying experiences on working finite element analysis in isotropic materials to laminated composites should be undertaken with care. It is our intent to address the effect of the composite ply stresses due to element meshing, boundary constraints and 2D versus 3D used in the modeling a composite structure.

Examples used in this study indicates special characteristics of composite structures such as symmetrical versus unsymmetrical laminate configurations and presence of edge stress need to be considered in application laminate configurations of finite element method to composite structures. The following address specific effects on stress results of finite element analysis on the issues mentioned before:

1. Element Meshing

The convergence of the ply stress due to the element aspect ratio is more pronounced for 00 ply than for the other angle ply. The element aspect ratio plays more important role on the ply stress for curved beam than for flat beam if the same type of element is used.

2. Boundary Constraints

Enforcing boundary constraints for symmetry needs to consider both structural configuration and material axis.

In 2D model, a full or a quarter model for symmetric and unsymmetrical laminate without a hole gives none or insignificant difference in the ply stress result. However, a quarter 2D model for unsymmetrical laminate with a hole gives significant difference than the results from a full 2D model.

For a laminate with a hole, a full and a quarter 3D models give significant different values of the peak stress. Moreover, using a quarter 2D or 3D model fails to predict the right location of the peak stress.

3. 2D versus 3D Model

The full 3D model of laminate without a hole gives lower in-plane stress than the 2D does, in particular at the edge of the laminate. A full 3D and full 2D model give a significant peak stress of each ply for laminate with a hole.

It is concluded that modeling a composite structure requires understanding the structural characteristics of composites.

APPENDIX A

FEM MODELS USED IN THE THESIS

ANSYS 11.0 has various solid elements like SOLID 182, SOLID 82, SOLID186, SOLID 45 etc. It is very important to choose proper element type for accurate results. SOLID 186 is a 20 node element with three degrees of freedom in each node. It is a higher order 3D element with quadratic displacement behavior. Since the stress field near the hole exhibits a high stress gradient, the higher order 3D element is a better candidate for analysis. Hence, SOLID 186 is chosen for the three dimensional finite element modeling. As Solid 186 was used for plate with a single hole model, we have used the same element for without hole model.

In process of doing the 3d modeling of a plate with a hole the first thing to do is to choose elements. Plane 183 and solid 186 were used here. Then material properties for orthotropic material were described. 2d geometry of the plate with single hole was created. The whole geometry was created in separate area and the area was glued together. This was done to create more dense mesh near the hole.

Local coordinate systems were created according to the lay-up of the composite material. For my coordinate system z axis will remain same as global coordinate. X axis and y axis will be along the fiber direction 1 and 2 respectively. It is to be noted that plane 183 cannot be used for curved beam models. The reason behind this is that it does not have the rotational degree of freedom that is necessary to model a curved beam. Any type of shell element can be used for that purpose. In the curved beam model in this thesis a Shell 99 element has been used for the curved beam surface. The following table will show the coordinate number designation and their angle of rotation with respect to global x coordinate. These coordinates in the three dimensional model will represent the fiber orientations.

Table A.1 Fiber orientation angle with respect to global x axis

designation	Rotation angle in degree
11	0
12	15
13	30
14	45
15	60
16	75
17	90
18	-15
19	-30
20	-45
21	-60
22	-75
23	-90

Then the whole area was selected and extruded with the thickness of single layup which is 0.005 inch and with the respective layup designation (if the lamina should be 45 deg of fiber direction the designated local coordinate system will be 14). During the extrusion SOLID 186 element was used. And after extrusion the 2d area underneath was deleted. In a similar fashion the whole geometry was created. The following figure will show the flow diagram of the modeling process.

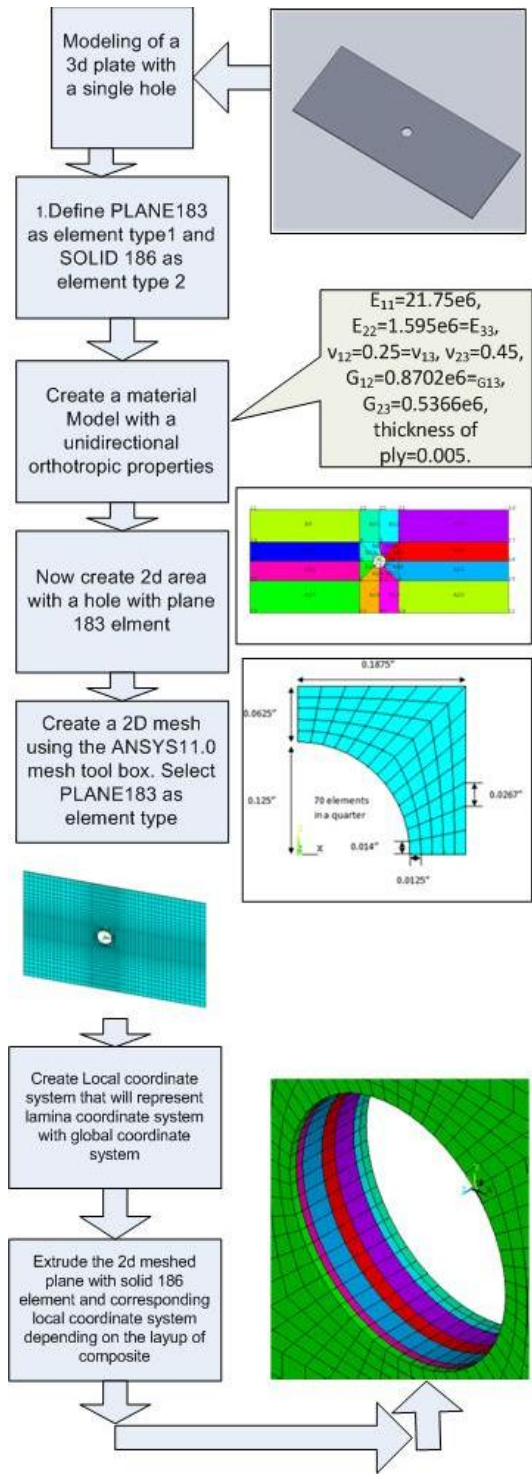


Figure A.1 Modeling technique flow diagram for 3D plate.

Two Dimensional Plate with a hole modeling will be discussed in the following section. A plate with a hole modeling technique will be discussed here of a layup of $[\pm 45/0/90]_s$. The geometry is 5inch*2inch*0.04 inch; circle diameter of 0.25 inch. For FEM model the element type used is Shell 99 layered element. After selecting the element the real constant set should be defined. In this set number of layer and the layer thickness will be defined. Ansys allows creating up to 250 layers. Here 8 layers were selected with given layup. For an example if the fiber direction is such that the 1 direction is 45 degree angled with the global coordinate, then the input will be 45 in degree. After defining the real constants the material constant should be defined. In this thesis an orthotropic material property ($E_{11}=21.75e6$, $E_{22}=1.595e6=E_{33}$, $\nu_{12}=0.25=\nu_{13}$, $\nu_{23}=0.45$, $G_{12}=0.8702e6=G_{13}$, $G_{23}=0.5366e6$, thickness of ply=0.005) has been used. Then the key points were created and through the key points areas were created. And created the solid circle ($r=0.125$) and subtract the circle from the areas. Then all the areas were glued together and mesh of proper choice was generated. After meshing it is to be ensured that all the elements have same element coordinate system. Now the geometry is ready to apply load and boundary conditions. The following figure will show the key points and the areas of a plate with a single hole.

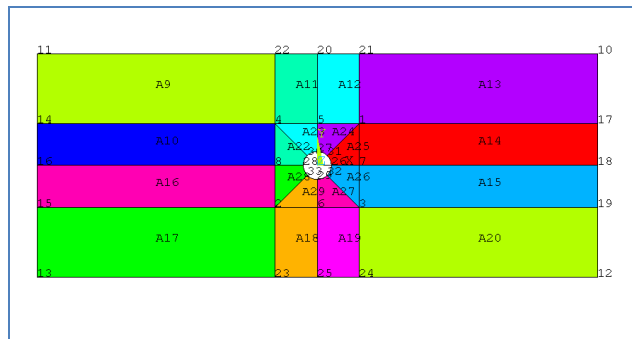


Figure A.2 Key points and Areas of a plate with a hole 2D model.

The following figure will show the step by step flow diagram of the modeling process. A flow model of a plate with a single hole has been shown here. An un-notched model can also be generated in the same manner.

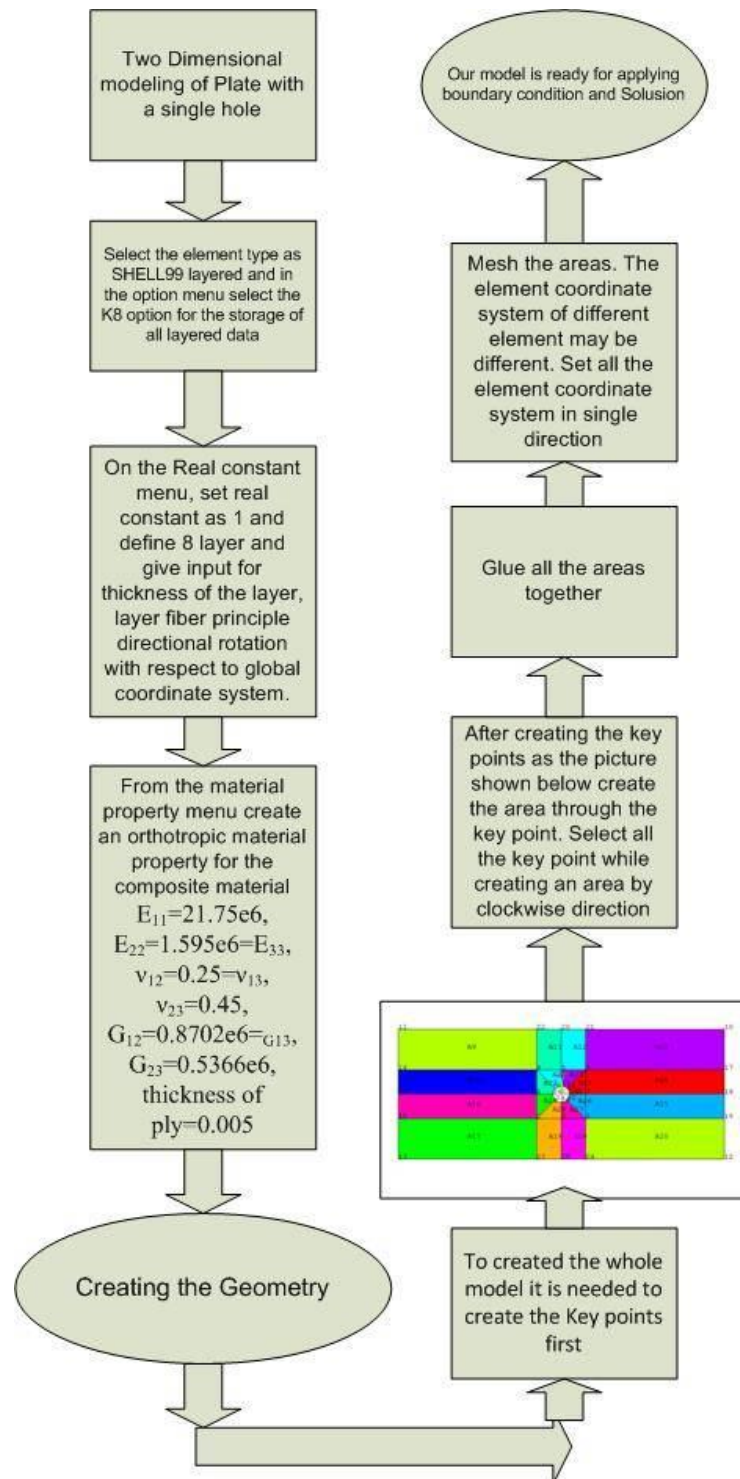


Figure A.3 Plate with a hole 2D model

In this section a three dimensional Curved beam modeling Process will be discussed. This modeling is more challenging than the 3D or 2D flat plate modeling. It is not possible to use PLANE 183 8 node element because it does not have any shear properties. So FEM modeling a shell element and a solid 186 element has been used. To model the curved surface PROE wildfire has been used. Ansys is used for creating the three dimensional geometry. In PROE a Curved surface with a radius of 0.58 inch was created. Here $s=R*\theta$, and the length of the beam is $L=6*s$. After creating the curved surface it was imported to Ansys as an IGS file. It was defined as a Shell element and was mapped meshed. The whole plate area was offset 8 times with a offset distance of 0.005 inch along the normal to the plate. At the center of the circle of the curve that constitutes the beam all the local coordinate system was defined. Each plate was extruded with the corresponding local coordinate designation and SOLID186 element along the normal of the plate and then the area underneath was deleted.

The following figure will show the step by step process of a three dimensional curved beam modeling technique. It is to be noted that for a curved beam the aspect ratio effect is of much concern in comparison to a flat plate modeling. So while modeling a proper aspect ratio and element size has to be chosen. While importing the IGS file in Ansys much care is needed. Ansys numbering control option is of a great help in order to minimize the node numbers and key point numbers.

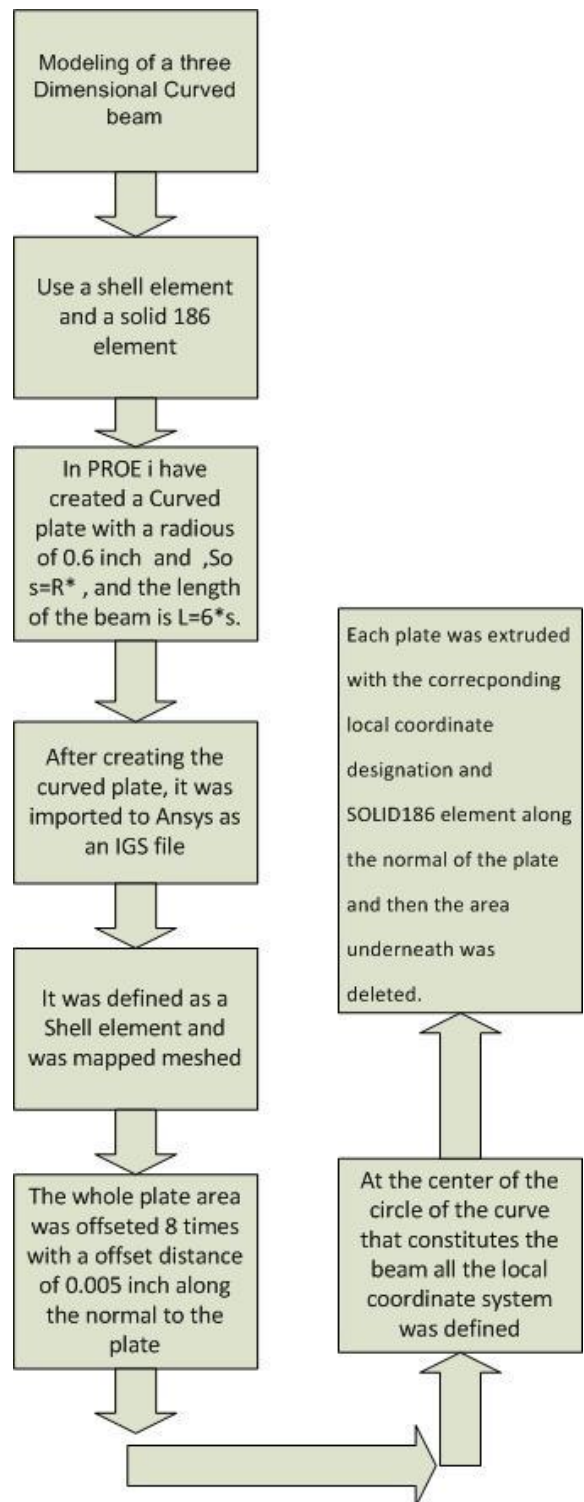


Figure A.4 Three dimensional Curved Beam

This section will describe the modeling technique of a two Dimensional curved beam. For two dimensional Curved Beam modeling a layered element, which consists of all the layers through the laminated thickness, is commonly used. For modeling of the curved beam SHELL99 layered element was used. The material constants, the layer fiber orientation and stacking sequence are directly input in the software (Ansys 11). A curved surface with accurate curvature was created by PROE and then transferred to the fem software as IGS file format. Then the curved surface was meshed using the SHELL99 element.

APPENDIX B

LAMINATION THEORY PROGRAM WRITTEN IN MATLAB FOR FLATE PLATE AND
CURVED BEAM

ABD MATRIX FORMULATION FUNCTION

```
function [ABDMat]=abd(E1,E2,G12,v12,tply,n,theta)
%clc;
s11=1/E1;    s12=-v12/E1;  s16=0;  s21=s12;  s22=1/E2;  s26=0;  s61=s16;
s62=s26;  s66=1/G12;

S=[s11 s12 s16;
   s21 s22 s26;
   s61 s62 s66];

Q=inv(S);%this will give q11 q12 q13.....same for all laminate
;gives 1 and 2 dimension values.

%//////////now we will calculate the Qbar matrix for all laminate and
keep
%them in a 12/3 matrix

L=0;% L will have discrete value 0,4,9,13...
QBAR=zeros(3*n,3);
%PART1 assembling total QBAR matrix for whole lamina
for i=1:n

    m1=cos(-theta(i)*(pi()/180));
    n1=sin(-theta(i)*(pi()/180));
    m2=cos(theta(i)*(pi()/180));
    n2=sin(theta(i)*(pi()/180));
```

```

    Tsigmatheta=[m1^2 n1^2 2*m1*n1; n1^2 m1^2 -2*n1*m1;-m1*n1 m1*n1
m1^2-n1^2];
    Tepsilontheta=[m2^2 n2^2 m2*n2; n2^2 m2^2 -n2*m2;-2*m2*n2 2*m2*n2
m2^2-n2^2];

```

```

    Qbar=Tsigmatheta*Q*Tepsilontheta;

```

```

        for j=1:3 %row
            for k=1:3%column

```

```

QBAR(j+L,k)=Qbar(j,k);%QBAR is taking the value of Qbar Q11 Q12 Q13
            end
        end
        %Q21 Q22 Q23

```

```

L=L+3;%go to the next lamina
end

```

```

%%%%%%%%%%%%%%%%%%%%%%%%%%%%%%%%%%%%%%%%%%%%%%%%%%%%%%%%%%%%%%%%%%%%%%%%%%upto this section i have stored my whole qbar
%matrixin a 12/3 matrix

```

```

%PART2

```

```

h=zeros(n+1,1);%a single column matrix of 5 zero element

```

```

L=0;
t=0;

```



```

for    i=1:n+1
        h(i)=(L-(n/2))*tply;%h1 is the lowest lamina A=Q*(h1-h2)
        L=L+1;
end

%////////////////////////////////////Coordinate difining is
%finished////////////////////////////////////

%PART3 THE A B D MATIX

A=zeros(3,3);%defining a 3/3 matrix whose components are zero

B=zeros(3,3);%defining a 3/3 matrix whose components are zero

D=zeros(3,3);%defining a 3/3 matrix whose components are zero

t=n+1;%t=5,4,3...
L=0;
for k=1:n
    for i=1:3
        for j=1:3
            A(i,j)=A(i,j)+QBAR(i+L,j)*(h(t)-h(t-1));
            B(i,j)=B(i,j)+(1/2)*QBAR(i+L,j)*(h(t)^2-h(t-1)^2);
            D(i,j)=(D(i,j)+(1/3)*QBAR(i+L,j)*(h(t)^3-h(t-1)^3));
        end
    end
end

L=L+3;
t=t-1;

```

```

end

%%%%%%%%%%%%%%%%%%%%%%%%%%%%%%%%%%%%%%%%%%%%%%%%%%%%%%%%%%%%%%%%%%%%%%%%%%%%%%
ABD=zeros(6,6);
L=3;
for i=1:3
    for j=1:3
        ABD(i,j)=A(i,j);
    end
end

for i=1:3
    for j=1:3
        ABD(i,j+L)=B(i,j);
        ABD(i+L,j)=B(i,j);
    end
end

for i=1:3
    for j=1:3
        ABD(i+L,j+L)=D(i,j);
    end
end

ABDMat=zeros(6,6);

```

```

a=[A zeros(3,3);zeros(3,6)];
b=[zeros(3,6);B zeros(3,3)];
c=[ zeros(3,3) B;zeros(3,6)];
d =[zeros(3,6) ;zeros(3,3) D];
ABDMat=(a+b+c+d);

```

. MID PLANE STRAIN CALCULATION FUNCTION

```

%mid plane strain and kuravature
function [strn]=midplane(E1,E2,G12,v12,tply,n,theta,NM)
NMM=[NM(1);NM(2);NM(3);NM(4);NM(5);NM(6)];

ABDMat=abd(E1,E2,G12,v12,tply,n,theta)%calling function abd
strn=ABDMat\NMM;

```

. STRESS CALCULATION

```

clc;
%%PART1
% define material properties
E1=21.75e6; E2=1.595e6; G12=0.8702e6; v12=0.25; tply=0.005;n=8;
s11=1/E1; s12=-v12/E1; s16=0; s21=s12; s22=1/E2; s26=0; s61=s16;
s62=s26; s66=1/G12;

```

```

%define layup and load
theta=[+45;45;-45;-45;90;90;0;0];
NM=[40;0;0;0;0;0];

%find strain and curvature(k)at mid plane
midstr=midplane(E1,E2,G12,v12,tply,n,theta, NM);

% Calculate ABD matrix from the abd funtion
ABDMat=abd(E1,E2,G12,v12,tply,n,theta);
abdmat=inv(ABDMat);
%segrigating a,b,c matrix
a=zeros(3,3);
b=zeros(3,3);
d=zeros(3,3);
for i=1:3
    for j=1:3
        a(i,j)=abdmat(i,j);
        b(i,j)=abdmat(i,j+3);
        d(i,j)=abdmat(i+3,j+3);
    end
end
end

%%PART 1 finished-----

%% Finding QBAR matrix for all layers: PART 2
S=[s11 s12 s16;
    s21 s22 s26;
    s61 s62 s66];

Q=inv(S);

L=0;% L will have discrete value 0,4,9,13...

```

```

QBAR=zeros(3*n,3);
%NOTE:PART2 assembling total QBAR matrix for whole lamina
for i=1:n

    m1=cos(-theta(i)*(pi()/180));
    n1=sin(-theta(i)*(pi()/180));
    m2=cos(theta(i)*(pi()/180));
    n2=sin(theta(i)*(pi()/180));

    Tsigmatheta=[m1^2 n1^2 2*m1*n1; n1^2 m1^2 -2*n1*m1;-m1*n1 m1*n1
m1^2-n1^2];
    Tepsilontheta=[m2^2 n2^2 m2*n2; n2^2 m2^2 -n2*m2;-2*m2*n2 2*m2*n2
m2^2-n2^2];

    Qbar=Tsigmatheta*Q*Tepsilontheta;

    for j=1:3 %row
        for k=1:3%column

            QBAR(j+L,k)=Qbar(j,k);

        end
    end

L=L+3;%go to the next lamina
end

%////////////////////////////////////upto this section i have stored my whole qbar
%matrixin a 12/3 matrix
%Finished PART 2
%% LAYER DISTANCE FROM MID PLANE

```

```

%PART3: Defining layer distance from midplane
h=zeros(n+1,1);
L=0;
t=0;
for i=1:n+1
    h(i)=(L-(n/2))*tply;%h1 is the lowest lamina A=Q*(h1-h2)
    L=L+1;
end

%%%%%%%%%%%%%%%%%%%%%%%%%%%%%%%%%%%%%%%%%%%%%%%%%%%%%%%%%%%%%%%%%%%%%%%%Coordinate difining is
%finished(Part3)%%%%%%%%%%%%%%%%%%%%%%%%%%%%%%%%%%%%%%%%%%%%%%%%%%%%%%%%%%%%%%%%%%%%%%%%

eps_0=zeros(3,1);
kapa=zeros(3,1);

%% LAYER STRESS CALCULATION

%for 45 deg layer
Qbar_45=zeros(3,3);
for i=1:3
    for j=1:3
        Qbar_45(i,j)=QBAR(i,j);
    end
end
eps_0(i)=midstr(i);
kapa(i)=midstr(i+3);
end
Str_45= Qbar_45*eps_0+h(9)*Qbar_45*kapa

%%for neg45 deg layer
Qbar_neg45=zeros(3,3);
for i=1:3

```

```

    for j=1:3
        Qbar_neg45(i,j)=QBAR(i+3,j);
    end
eps_0(i)=midstr(i);
kapa(i)=midstr(i+3);
end
Str_neg45=Qbar_neg45*eps_0+h(8)*Qbar_neg45*kapa

%%for 0 deg layer
Qbar_0=zeros(3,3);
for i=1:3
    for j=1:3
        Qbar_0(i,j)=QBAR(i+6,j);
    end
eps_0(i)=midstr(i);
kapa(i)=midstr(i+3);
end
Str_0=Qbar_0*eps_0+h(7)*Qbar_0*kapa

%%for 90 deg layer
Qbar_90=zeros(3,3);
for i=1:3
    for j=1:3
        Qbar_90(i,j)=QBAR(i+9,j);
    end
eps_0(i)=midstr(i);
kapa(i)=midstr(i+3);
end
Str_90=Qbar_90*eps_0+h(6)*Qbar_90*kapa

%%for Sec90 deg layer
Qbar_sec90=zeros(3,3);

```

```

for i=1:3
    for j=1:3
        Qbar_sec90(i,j)=QBAR(i+12,j);
    end
eps_0(i)=midstr(i);
kapa(i)=midstr(i+3);
end
Str_sec90=Qbar_sec90*eps_0+h(5)*Qbar_sec90*kapa

%%for Sec0 deg layer
Qbar_sec0=zeros(3,3);
for i=1:3
    for j=1:3
        Qbar_sec0(i,j)=QBAR(i+15,j);
    end
eps_0(i)=midstr(i);
kapa(i)=midstr(i+3);
end
Str_sec0=Qbar_sec0*eps_0+h(4)*Qbar_sec0*kapa

%%for Secneg45 deg layer
Qbar_secneg45=zeros(3,3);
for i=1:3
    for j=1:3
        Qbar_secneg45(i,j)=QBAR(i+18,j);
    end
eps_0(i)=midstr(i);
kapa(i)=midstr(i+3);
end
Str_secneg45=Qbar_secneg45*eps_0+h(4)*Qbar_secneg45*kapa

%%for Sec45 deg layer

```



```
Qbar_sec45=zeros(3,3);
for i=1:3
    for j=1:3
        Qbar_sec45(i,j)=QBAR(i+21,j);
    end
eps_0(i)=midstr(i);
kapa(i)=midstr(i+3);
end
Str_sec45=Qbar_sec45*eps_0+h(3)*Qbar_sec45*kapa
%finish
```

REFERENCES

1. O. O. Ochoa and J. N. Reddy, "Finite Element Analysis of Composite Laminates" Published by Kluwer Academic Publishers, 1992
2. F. L. Matthews, G. A. O. Davis, D Hitchings and C Soutis, "Finite Element Modelling of Composite Materials and Structures", WoodHead Publications Limited,
3. Ever J. Barbero, "Finite Element Analysis of Composite Materials", CRC Press Taylor and Francis Group, Aug03,
4. D. J. Chen and W. S. Chan., "Use of Composite Effective Moduli for Lumping Layers in Finite Element Analysis", Proceedings of the 37TH AIAA SDM Conference, Salt Lake City, Utah, April 15-17, 1996.
5. Chan, W. S., Lin, C. Y., Liang Y. C. and Hwu., C., "Equivalent Thermal Expansion Coefficient of Lumped Layer in Laminated Composites", Composites Science and Technology 66 (2006) 2402–2408
6. Issac M. Daniel and Ori Ishahi, "Engineering Mechanics of Composite materials". Second edition, 2006.
7. K. A. Syed; C. W. Su; W. S. Chan, "Analysis of Fiber-Reinforced Composite Beams Under Temperature Environment", Journal of Thermal Stresses, 1521-074X, Volume 32, Issue 4, 2009, Pages 311 – 321
8. Thien H Nguyen, "Effects of curvature on the stresses of a laminated curved beam subjected to bending", Department of Mechanical and Aerospace Engineering, University of Texas at Arlington, May 2006.
9. J.N. Reddy, "An Introduction To The Finite Element Method", Second Edition 1993.

10. Doe Jhon Chen, "Efficient Finite Element Analysis of Composite Laminate", Department of Mechanical and Aerospace Engineering, University of Texas at Arlington, December, 1995.
11. Syed, K. A., and Chan, W. S., "Analysis of Hat-Sectioned Reinforced Composite Beams", Proceedings of American Society for Composites Conference.
12. Rios, G. F. and Chan W. S., "A unified Analysis of Stiffener Reinforced Composite Beam with Arbitrary Cross-section", 2009, Department of Mechanical and Aerospace Engineering, University of Texas at Arlington.

BIOGRAPHICAL INFORMATION

Farhan Alamgir received his B.S in mechanical engineering from the Bangladesh University of Engineering and Technology in 2004. He completed his master's of engineering degree in mechanical engineering at the University of Texas at Arlington in 2011.

Farhan served as Plant engineer in two of the major Power Plants (AES Haripur 360 MW CCPP and GLOBELEQ Meghnaghat 450 MW CCPP) for four years.